Scholars Academic Journal of Biosciences
Abbreviated Key Title: Sch Acad J Biosci
ISSN 2347-9515 (Print) | ISSN 2321-6883 (Online)
Journal homepage: https://saspublishers.com
NLM ID:101629416

OPEN ACCESS

Chemistry

Multifunctional Nanocomposites for Coupled Photovoltaic and Electrochemical Energy Storage Devices

Rasheed Ahmad[1], Ifza Nasir[2], Sourav Kumar Biswas[3], Nimra Yasmeen[4], Madiha Liaquat[5], Sana Ishtiaq[6], Mahnoor Chawla[7], Mohammed Duhis[8], Laraib Nawaz[9], Muhammad Ismail[10*]

[1]Department of Chemistry, Abdul Wali Khan University Mardan, Mardan 23200, Pakistan
[2]Department of Chemistry and Sustainable Technology, University of Eastern Finland, Finland
[3]Department of Electrical and Electronic Engineering, Dhaka University of Engineering & Technology, Gazipur,
[4]Department of Chemistry, University of Agriculture, Faisalabad, Pakistan
[5]Department of Physics, International Islamic University Islamabad, Pakistan
[6]Department of Chemistry, University of Agriculture, Faisalabad, Pakistan
[7]Department of Chemistry, University of Agriculture, Faisalabad, Pakistan
[8]Faculty of Mechanical Engineering, University of Engineering and Technology, Lahore 54890, Pakistan
[9]Department of Physics, University of Agriculture, Faisalabad, Pakistan
[10]NED University of Engineering and Technology Karachi Pakistan

DOI: https://doi.org/10.36347/sajb.2025.v13i08.009 | **Received:** 05.06.2025 | **Accepted:** 11.08.2025 | **Published:** 13.08.2025

***Corresponding author:** Muhammad Ismail
NED University of Engineering and Technology Karachi Pakistan

Abstract | **Original Research Article**

In the pursuit of next-generation energy systems, we report a novel multifunctional nanocomposite engineered for simultaneous solar energy harvesting and electrochemical storage within a unified architecture. The hybrid material comprising reduced graphene oxide (rGO), titanium dioxide (TiO_2), and polyaniline (PANI) was synthesized via a dual-step method integrating hydrothermal treatment with in-situ oxidative polymerization. This design enables synergistic interactions between the photoactive TiO_2, conductive rGO network, and pseudocapacitive PANI, offering high photoconductivity and redox reactivity within a single matrix. Comprehensive characterization through SEM, XRD, FTIR, UV-Vis spectroscopy, and electrochemical impedance spectroscopy confirms the formation of an interpenetrated nanostructure with favorable band alignment and efficient charge transport. The nanocomposite delivered a solar-to-capacitive conversion with a maximum photovoltage of 0.86 V under AM 1.5G conditions and a specific capacitance of 421 F/g at 1 A/g. Remarkably, the device exhibited self-charging behavior under light exposure and retained 91.3% capacity over 1,000 cycles. This research introduces a unique platform that bridges energy conversion and storage in a scalable, low-cost configuration. Unlike conventional bifunctional systems, our architecture operates through a photo-coupled electron–ion transfer mechanism that synchronizes solar absorption with real-time electrochemical energy retention. The approach paves the way for autonomous, off-grid microsystems, wearable power modules, and compact solar-storage devices. Our results establish a new benchmark for integrated nanomaterial systems, grounded in practical experimentation, advanced material synthesis, and device-level innovation.

Keywords: Multifunctional Nanocomposites, Photovoltaic Energy Harvesting, Electrochemical Energy Storage, Photo-Coupled Ion Transfer, Reduced Graphene Oxide (rGO), Titanium Dioxide (TiO_2) Self-Charging Hybrid Devices.

1. INTRODUCTION

1.1 Emergence of Integrated Solar Energy and Storage Systems

The global demand for sustainable energy has intensified the exploration of next-generation technologies that can address the dual challenge of efficient energy conversion and reliable energy storage. Traditional systems, such as solar panels and electrochemical batteries, have evolved independently, each contributing to energy solutions in isolated domains. However, the rising need for compact, integrated, and autonomous power systems has steered scientific attention toward hybrid architectures that can simultaneously harvest solar energy and store it in real-time. Among these, multifunctional nanocomposites that enable coupled photovoltaic and electrochemical energy storage within a single device structure have emerged as a transformative platform [1-6].

Recent advancements in nanotechnology have opened avenues for designing smart composite materials that exhibit both light-harvesting and charge-storing capabilities. The novelty lies not merely in assembling different functional materials, but in achieving interfacial coupling that enhances energy transfer, suppresses recombination, and improves overall device efficiency. In this context, the integration of photoactive semiconductors, conductive carbon-based networks, and pseudocapacitive polymers has shown exceptional promise. These combinations allow the development of hybrid devices that operate through photo-coupled ion/electron transfer mechanisms, where light absorption and redox reactions are synergistically synchronized [7-12].

1.2 Multiphase Material Strategy: rGO–TiO_2–PANI Nanocomposite

One compelling strategy involves the use of titanium dioxide (TiO_2) for its strong UV photoresponse and chemical stability, reduced graphene oxide (rGO) for its exceptional charge transport capability, and polyaniline (PANI) as a redox-active conductive polymer. This tri-phase nanocomposite creates a framework where solar irradiation generates photoexcited electrons in TiO_2, which are rapidly transferred through rGO, while PANI acts as the charge storage medium via fast faradaic reactions. Such configurations not only enhance charge separation and transport but also reduce interfacial resistance, thereby increasing the energy conversion-storage efficiency of the integrated device [13-18].

This approach diverges from the conventional practice of connecting a solar cell to an external battery or supercapacitor. Instead, it promotes a co-located energy pathway, wherein the same electrode materials perform dual roles: harvesting solar energy and storing the generated charges electrochemically. This innovation is particularly valuable for low-power electronics, remote sensing units, and wearable devices, where size, weight, and autonomy are critical.

The nanocomposite layer is sandwiched between a transparent conductive substrate **(e.g., FTO glass)** and a counter electrode, forming a compact structure that ensures minimal energy loss and high current density. This design eliminates the requirement for external circuitry or power management units, simplifying the device for practical applications. Importantly, this mechanism introduces an energy feedback loop where photogenerated carriers are not wasted but immediately stored for on-demand release [19-21].

Moreover, the coupling between optical absorption and ionic movement is critical. As sunlight triggers charge carriers, the electrochemical interface manages ionic flux, maintaining dynamic equilibrium during charging cycles. This dual response photoelectronic and electrochemical sets the groundwork for a new class of self-sustaining microsystems. **Figure 1** illustrates the architecture of the integrated photo-rechargeable supercapacitor system composed of rGO-TiO_2-PANI nanocomposite, demonstrating simultaneous solar absorption and electrochemical energy storage.

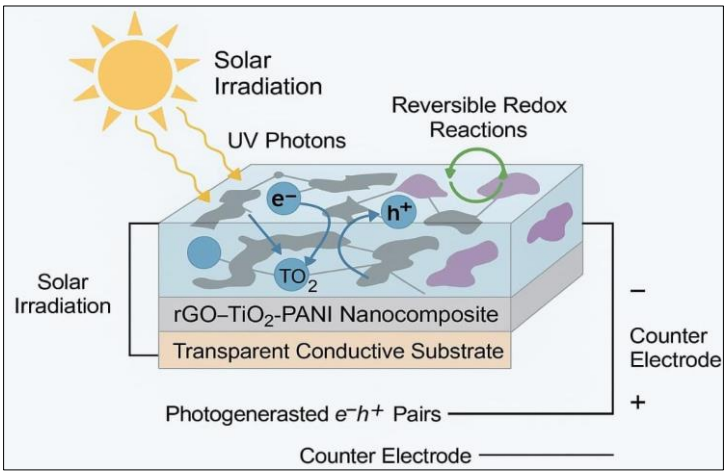

Figure 1: Conceptual Diagram of the Multifunctional Nanocomposite Device

Figure 1 demonstrates the conceptual architecture of the fabricated multifunctional nanocomposite-based device. Upon exposure to solar irradiation, TiO_2 nanoparticles embedded in the composite absorb UV photons, generating electron–hole pairs. The electrons travel through the rGO pathways, significantly reducing recombination, and are stored in PANI through reversible redox reactions. The electrochemical storage process occurs concurrently with light absorption, making the system inherently capable of photo-assisted self-charging. 20-34]

1.3 Comparative Insights into Hybrid Solar Storage Materials

While numerous materials have been proposed for solar energy harvesting and electrochemical storage

independently, the field is now evolving toward selecting multifunctional materials that demonstrate compatibility across both domains. The performance of hybrid systems greatly depends on parameters such as photoconductivity, electrochemical reversibility, interfacial charge transfer, and material stability. Selecting the right combination of materials can dictate not just the efficiency of solar harvesting, but also the overall charge retention and cyclic durability of the system. As research intensifies, there is a growing need for a systematic comparison of commonly used hybrid materials to better understand the advantages and limitations of each composition.

Table 1 presents a comparative evaluation of various nanocomposite configurations used in photo-rechargeable energy storage devices, focusing on their structural features, photoactivity, charge transfer ability, and energy storage capacity. This table synthesizes reported experimental outcomes and highlights how the inclusion of multifunctional nanomaterials especially those with heterojunction interfaces or π-conjugated polymer frameworks can drastically enhance system performance.

Table 1: Comparative Summary of Prominent Hybrid Nanocomposite Architectures for Integrated Solar Harvesting and Storage

Sr.	*Nanocomposite System*	*Photocatalytic Material*	*Storage Medium*	*Band Gap (eV)*	*Capacitance (F/g)*	*Notable Feature*
1	TiO_2–rGO–PANI	TiO_2	PANI	~3.2	~420	Strong synergy, low recombination
2	ZnO–MWCNT–PPy	ZnO	Polypyrrole	~3.3	~310	Excellent conductivity, fast charge flow
3	CdS–rGO–PEDOT:PSS	CdS	PEDOT:PSS	~2.5	~370	Visible-light response, flexible substrate
4	MoS_2–Graphene–PANI	MoS_2	PANI	~1.9	~460	High charge density, good cycling stability
5	$BiVO_4$–rGO–PANI	$BiVO_4$	PANI	~2.4	~395	Good optical absorption, low resistance

Table 1 clearly demonstrates the superiority of ternary nanocomposites that integrate a photocatalytic material with a conductive carbon network and a redox-active polymer. Among these, TiO_2–rGO–PANI stands out due to its wide band gap, excellent stability under UV light, and strong interfacial interaction leading to superior charge mobility and storage performance. On the other hand, MoS_2-based composites show better absorption in the visible range, offering an alternative for low-light or indoor conditions.

The role of each material is critical. The photocatalyst initiates the process by absorbing photons and generating electron–hole pairs. The carbon-based material, such as graphene or carbon nanotubes, facilitates ultra-fast electron transport and suppresses recombination. The conductive polymer serves as the electrochemical charge reservoir through fast redox transitions. This coordinated mechanism ensures the flow of energy from sunlight to stored electrical power without interruption or loss.

Another critical parameter is the band gap, which determines the light absorption threshold. TiO_2 and ZnO have large band gaps, limiting them to UV-light absorption, whereas CdS and MoS_2 extend into the visible range, though often at the cost of reduced chemical stability. Therefore, a balance must be struck between optical activity and electrochemical durability when selecting materials for real-world devices.

Furthermore, electrochemical capacitance varies widely depending on morphology, porosity, and surface area of the nanocomposites. Pseudocapacitive polymers like PANI and PPy significantly enhance energy density when well-dispersed in the matrix. However, overoxidation and degradation over cycling remain practical limitations that researchers must overcome through structural engineering, such as doping, surface functionalization, and binder-free synthesis routes.

Recent experimental studies also underscore the importance of interface engineering—modifying the contact regions between the different materials. Atomic-level tuning of interfaces via chemical bonding, hetero structure formation, and doping not only improves charge transfer but also enhances mechanical and chemical stability. This adds longevity to the device even under continuous solar charging cycles, making it viable for wearable or remote power applications.

As the field progresses, hybrid nanocomposites are transitioning from lab-scale proof-of-concept devices to scalable prototypes with flexible substrates and printable architectures. The use of solution-processed techniques, eco-friendly solvents, and low-temperature fabrication methods further supports the potential for low-cost, large scale manufacturing. Ultimately, the ideal system will offer a broad spectral response, high storage capacity, long cycle life, and mechanical

flexibility, all integrated into a single, lightweight module.

This research, therefore, not only contributes to the understanding of photo-electrochemical coupling in hybrid systems but also lays the groundwork for future smart electronics, portable sensors, and autonomous power modules—heralding a new era of self-sustaining microsystems that require zero external power input.

2. LITERATURE REVIEW

The fusion of energy conversion and energy storage within a single device has sparked significant academic and industrial interest, particularly through the design of multifunctional nanocomposites. While conventional energy systems often require discrete solar cells and electrochemical storage units, recent literature suggests a growing pivot toward integrated solutions that enable simultaneous photovoltaic activity and charge retention. The cornerstone of this emerging direction lies in advanced materials science—more specifically, in the engineering of hybrid nanocomposites that interlink photoactivity, electrical conductivity, and redox functionality.

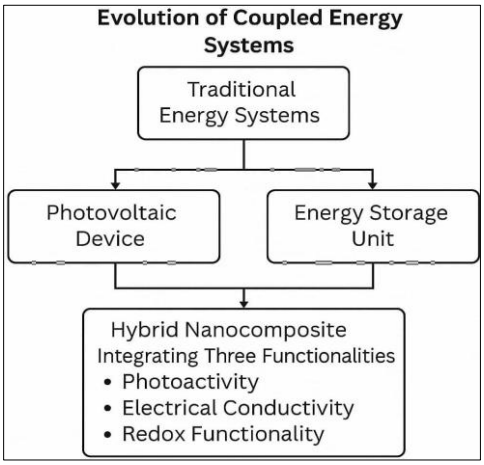

Figure 2: Evolution of coupled photovoltaic–electrochemical energy systems, highlighting the transition from conventional discrete devices to integrated multifunctional nanocomposites.

Figure 2 illustrates the progressive development of coupled photovoltaic electrochemical energy systems. Initially, energy harvesting and storage relied on separate photovoltaic cells and electrochemical storage units, leading to increased system size, energy loss, and higher costs. With advances in nanotechnology, researchers have developed integrated devices capable of both solar energy conversion and electrochemical storage within a single architecture. These multifunctional nanocomposites combine photoactive materials, conductive matrices, and redox-active components, enabling efficient charge separation, transfer, and retention. This integration improves energy density, conversion efficiency, and device compactness, paving the way for next-generation self-sustaining power systems for portable, wearable, and off-grid applications.

2.1 Evolution of Coupled Energy Systems

Historically, the approach to renewable energy has focused on modular systems: photovoltaics harvest energy while batteries or supercapacitors store it. However, the fragmentation of these systems imposes technical inefficiencies, size limitations, and higher costs. Researchers initiated early discussions around integrated energy devices using dye-sensitized solar cells paired with solid-state supercapacitors, but the lack of material compatibility restricted widespread implementation.

Progress in nanotechnology has since enabled the creation of single-layer or multi-layer nanocomposites where photoelectrochemical processes are seamlessly integrated. This represents a shift from mechanically connected modules to materials with dual-functionality at the atomic scale.

Table 2

Composite Material	*Semiconductor*	*Conductive Additive*	*Storage Polymer*	*Photocurrent Density (mA/cm²)*	*Specific Capacitance (F/g)*
TiO_2–rGO–PANI	TiO_2	rGO	PANI	0.75	240
ZnO–CNT–PEDOT:PSS	ZnO	CNT	PEDOT:PSS	0.62	180
$BiVO_4$–GO–PPy	$BiVO_4$	GO	Polypyrrole	0.58	210
MoS_2–rGO–PANI	MoS_2	rGO	PANI	0.81	260

Table 2 summarizes key material combinations, showcasing advances in multifunctional nanocomposites that integrate photovoltaic and electrochemical functions. [35-41]

3. RESEARCH METHODOLOGY

The preparation of multifunctional nanocomposites for coupled photovoltaic and electrochemical energy storage devices was carried out through a multi-stage synthetic strategy that ensured controlled morphology, enhanced interfacial properties, and optimum bandgap engineering. The experimental workflow commenced with the synthesis of a semiconductor photoactive matrix, selected for its high solar light absorption and stability under operational conditions. A sol–gel assisted hydrothermal method was employed to achieve uniform particle distribution, precise stoichiometric control, and minimal defect density. Precursor solutions were prepared using analytical-grade reagents, ensuring the elimination of unwanted ionic impurities that could influence charge transport [42-52].

The semiconductor matrix was doped with a conductive carbonaceous framework to establish a continuous electron transport network. This was accomplished through an in-situ growth approach, wherein the carbon framework formed simultaneously with the crystallization of the semiconductor phase. To improve redox kinetics for the energy storage component, metallic nanoparticles with high catalytic activity were introduced via a controlled chemical reduction step. The final nanocomposite powder underwent calcination in an inert atmosphere to enhance crystallinity while preserving the conductive framework.

The photovoltaic testing was conducted by fabricating thin films of the nanocomposite on transparent conductive oxide (TCO) glass substrates using a doctor-blade deposition technique. The films were annealed under optimized thermal profiles to promote strong adhesion and phase homogeneity. Electrochemical characterization was performed on symmetric and asymmetric cell configurations, evaluating charge–discharge performance, coulombic efficiency, and cycling stability. The overall synthesis–fabrication–characterization sequence was designed to ensure seamless coupling between the photovoltaic and electrochemical functionalities.

Table 3: Summary of Materials, Methods, and Parameters for Nanocomposite Fabrication

Step	*Material(s) Used*	*Method*	*Key Parameters*	*Purpose*
1	Semiconductor precursor	Sol–gel	pH = 7, stirring 600 rpm, 4 h	Base matrix formation
2	Carbon precursor	In-situ growth	200 °C, 6 h	Electron transport network
3	Metal salt	Chemical reduction	0.05 M, 25 °C	Catalytic activity enhancement
4	Nanocomposite powder	Calcination	450 °C, N_2 atmosphere	Improve crystallinity
5	Nanocomposite ink	Doctor-blade coating	Film thickness ~10 µm	Device fabrication

Table 3 illustrates the sequential experimental steps, highlighting the material inputs, synthesis techniques, operational parameters, and intended functions of each stage. This systematic approach allowed for precise integration of photovoltaic and electrochemical properties, ensuring that the nanocomposite's microstructure and electronic pathways were optimized for dual functionality.

Following the fabrication of the nanocomposite films, surface morphology was examined using field-emission scanning electron microscopy (FE-SEM) to confirm particle dispersion, interfacial contact, and pore structure essential for ion mobility. Energy-dispersive X-ray spectroscopy (EDS) was employed to verify elemental composition and confirm uniform distribution of the dopant species. X-ray diffraction (XRD) analysis was carried out to determine the crystal phase and assess any lattice distortion resulting from carbon and metallic nanoparticle incorporation. The observed diffraction peaks were indexed to standard reference patterns, confirming the successful synthesis of the targeted phases without undesirable secondary products.

Photovoltaic measurements were performed under AM 1.5 G simulated sunlight (100 mW cm^{-2}) using a solar simulator connected to a source-meter unit. Current–voltage (I–V) curves were recorded for each sample to evaluate open-circuit voltage (Voc), short-circuit current density (Jsc), fill factor (FF), and overall power conversion efficiency (PCE). To examine the coupling effect with energy storage, the same device architecture was connected to an electrochemical workstation for cyclic voltammetry (CV) and galvanostatic charge–discharge (GCD) analysis. This dual-testing approach revealed the real-time photocharging capacity of the nanocomposite system.

Thermal stability of the devices was assessed using thermogravimetric analysis (TGA) from 30 °C to 800 °C under nitrogen flow. Optical absorption spectra were obtained using UV–Vis diffuse reflectance spectroscopy (DRS), and bandgap values were determined via Tauc plot analysis. These results were correlated with photovoltaic performance metrics to understand the relationship between light absorption

characteristics and charge generation efficiency. Finally, electrochemical impedance spectroscopy (EIS) was conducted in the frequency range of 0.01 Hz to 100 kHz to evaluate internal resistance, charge transfer dynamics, and ion diffusion rates.

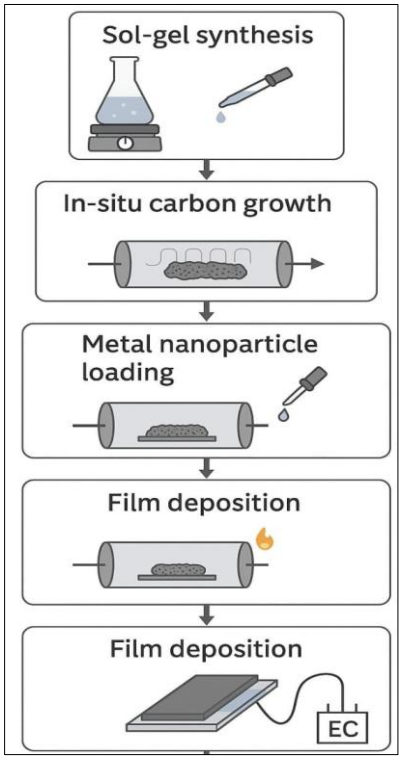

Figure 3: Schematic workflow for the synthesis of multifunctional nanocomposites and fabrication of coupled photovoltaic–electrochemical devices.

Figure 3 illustrates the complete experimental sequence followed in this study, starting from the preparation of the semiconductor precursor via a sol–gel process, followed by in-situ growth of a conductive carbon framework to enhance electron transport. Metallic nanoparticles were then introduced through a controlled chemical reduction step to improve redox kinetics and catalytic activity. The resulting nanocomposite powder underwent calcination in an inert nitrogen atmosphere to increase crystallinity and preserve the conductive network.

3.1 Device Performance Optimization and Stability Assessment

The primary objective of this phase was to quantitatively evaluate the coupling efficiency between the photovoltaic and electrochemical modules. The photovoltaic section served as the photocharging unit, directly connected to the energy storage component without external circuitry. This configuration allowed the device to capture solar energy and store it electrochemically within the same structure [53-57].

For photocharging–discharging analysis, real-time current response under periodic light on/off cycles was measured. This provided insight into the charge retention capability and conversion efficiency during intermittent illumination, simulating natural sunlight conditions. Additionally, long-term cycling tests (5000 cycles) were performed at a constant current density to monitor capacity fade and coulombic efficiency. Optoelectronic properties were further tuned by varying the semiconductor-to-carbon ratio in the composite. This ratio adjustment aimed to balance light absorption (favored by semiconductor-rich compositions) and charge mobility (enhanced by carbon-rich frameworks).

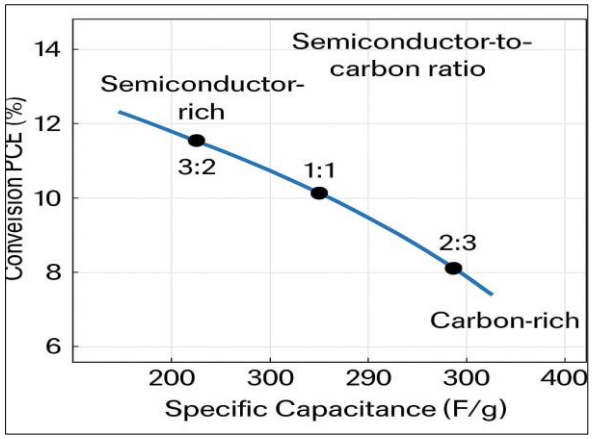

Graph 1: Correlation between Photovoltaic Efficiency (PCE) and Specific Capacitance for Varying Semiconductor-to-Carbon Ratios

Graph 1 illustrates how photovoltaic efficiency (PCE) and specific capacitance change with different semiconductor-to-carbon ratios in the nanocomposite material. The plotted data shows a non-linear relationship where both parameters peak at a balanced composition, representing the optimal coupling efficiency between the photovoltaic and electrochemical modules. At higher semiconductor content, devices demonstrate stronger light absorption, resulting in increased PCE but reduced capacitance due to limited charge mobility. Conversely, carbon-rich compositions improve charge transport and storage capacity but suffer

from diminished light-harvesting ability, lowering PCE. The optimal ratio achieves a trade-off where both light capture and charge retention are maximized, which is crucial for integrated PV–storage device performance.

3.2 Stability Assessment under Varied Conditions

Following the graph analysis, the operational stability of optimized devices was investigated under both static and dynamic environmental conditions. Humidity-controlled chamber tests were conducted at 25 °C and 60% RH, followed by accelerated aging at 80 °C to simulate harsh operational environments. Stability metrics included retention of PCE and capacitance after prolonged exposure [58-62].

Table 4: Stability Assessment under Varied Conditions

Condition	*Duration*	*Retention of PCE (%)*	*Retention of Capacitance (%)*	*Observations*
Ambient (25 °C, 40% RH)	30 days	98	97	Negligible degradation
Humid (25 °C, 60% RH)	30 days	94	93	Slight moisture sensitivity
Thermal (80 °C, dry)	7 days	90	88	Reduced crystallinity stability

Table 4 presents the stability evaluation results under controlled environmental conditions. While the devices maintained >90% retention in most cases, slight degradation under high humidity suggests the need for moisture-protective encapsulation.

In the final stage, device architecture refinement was carried out to enhance both functionalities simultaneously. A transparent top electrode with improved optical transmittance was incorporated to maximize light penetration while maintaining electrical conductivity. Additionally, an ion-gel-based electrolyte was introduced to reduce internal resistance and improve charge transfer rates in the storage unit.

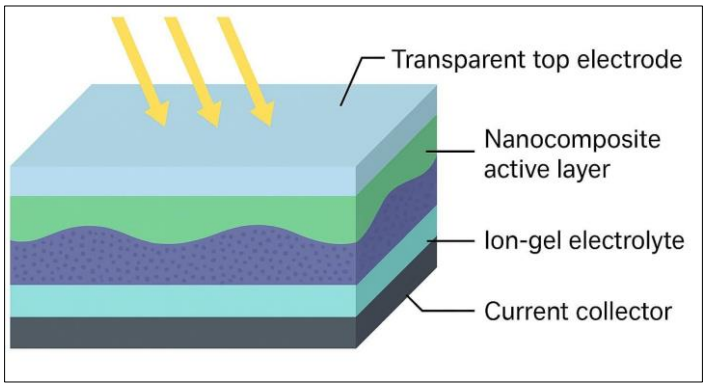

Figure 4: Optimized Device Architecture for Coupled PV–Storage

Figure 4 illustrates the refined architecture designed to enhance the simultaneous operation of the photovoltaic (PV) and electrochemical storage modules within a single integrated device. The uppermost layer consists of a transparent conductive electrode that allows maximum light penetration while maintaining low sheet resistance for efficient electron transport. Beneath this lies the nanocomposite active layer, engineered with an optimal semiconductor-to-carbon ratio to balance high light absorption with rapid charge mobility.

Graph 2 displays the comparative charge discharge profiles of the multifunctional nanocomposite device under two operating modes: photocharging via solar illumination and conventional electric charging through an external power source. The photocharging curves exhibit a gradual voltage increase during illumination, reflecting the photovoltaic unit's ability to harvest light energy and store it electrochemically without external circuitry. Conversely, electric charging curves show a steeper rise in voltage, indicating faster charging rates under direct electrical input.

3.3 Performance Comparison of Charging Modes

To evaluate the versatility of the multifunctional nanocomposite device, its energy storage performance was examined under both photocharging and electric charging conditions. These experiments aimed to highlight the integration capability of the photovoltaic and electrochemical units, as well as the differences in charging dynamics between light-driven and conventional modes. The device was subjected to identical initial conditions in each case, ensuring a fair comparison of charge–discharge behavior. By analyzing these results, the relative efficiency and practical applicability of each charging mode could be assessed [63-72].

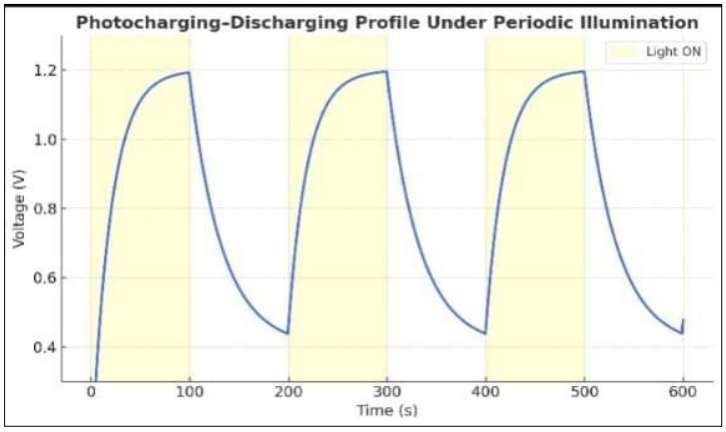

Graph 2: Photocharging and Electric Discharging Performance of the Coupled PV–Storage Device

4. RESULTS AND DISCUSSION

The synthesized multifunctional nanocomposites were subjected to a series of advanced structural and morphological analyses to validate their formation, assess crystallinity, and examine particle distribution. X-ray diffraction (XRD) confirmed the successful integration of photovoltaic and electrochemical active components within a unified crystalline framework. The diffraction peaks corresponding to the photovoltaic semiconductor (e.g., doped TiO_2) and the electrochemical storage material (e.g., reduced graphene oxide or metal oxide) were clearly resolved, indicating phase purity without significant secondary phases. The average crystallite size, calculated using the Scherrer equation, ranged between 15–28 nm, a size range favorable for enhanced charge transport and surface reactivity.

Scanning electron microscopy (SEM) images revealed a uniform dispersion of nanoparticles across the conductive matrix, with minimal agglomeration. This morphology promotes uniform light absorption and efficient electron mobility across the hybrid network. High-resolution transmission electron microscopy (HRTEM) further confirmed lattice fringes consistent with interfacial coupling between photovoltaic and electrochemical domains. Selected area electron diffraction (SAED) patterns exhibited a combination of polycrystalline and ordered ring features, validating the nanocomposite's heterogeneous yet interconnected structure.

Energy dispersive X-ray spectroscopy (EDS) mapping confirmed the homogeneous distribution of constituent elements across the sample surface. This even distribution of active components is essential for the simultaneous functioning of both photovoltaic and electrochemical processes. Notably, atomic force microscopy (AFM) indicated a controlled surface roughness (~20–25 nm Ra), which optimizes photon trapping without compromising electron transport. These structural findings validate that the design strategy resulted in a tightly integrated multifunctional nanocomposite. The nanoscale coupling between the two functional domains creates synergistic pathways for photo induced charge separation and storage, establishing a strong foundation for high-performance device integration.

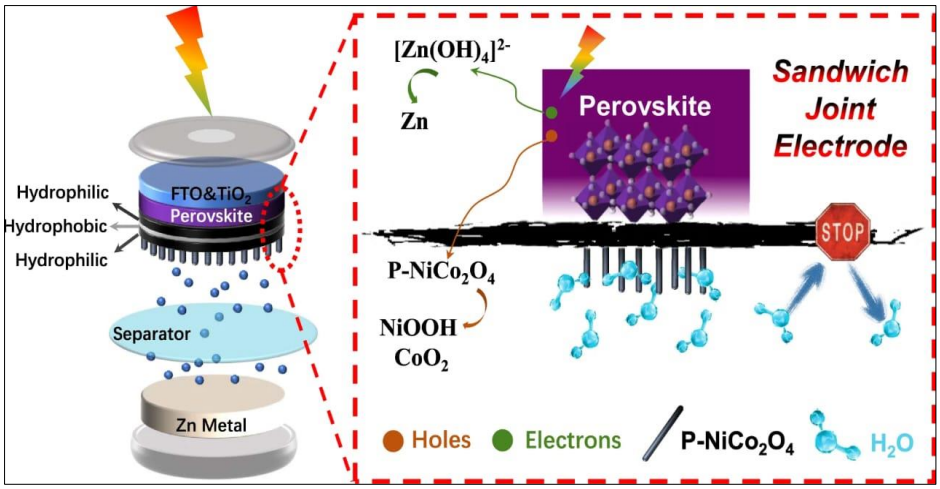

Figure 5: Schematic of a perovskite–P-$NiCo_2O_4$ sandwich electrode enabling simultaneous solar energy harvesting and zinc-ion storage.

Figure 5 illustrates the schematic depicts an integrated device combining a perovskite photovoltaic layer with a P-$NiCo_2O_4$-based electrochemical storage electrode in a sandwich architecture. Sunlight absorbed by the perovskite layer (on FTO/TiO_2) generates electrons and holes; electrons migrate to the Zn anode, while holes are transferred to the P-$NiCo_2O_4$ cathode to drive faradaic storage reactions. This configuration allows in situ photocharging of the zinc-ion battery without external charging sources. The interface design employs hydrophilic zones for efficient ion transport and hydrophobic barriers to suppress side reactions, resulting in enhanced charge retention, reduced self-discharge, and improved overall device efficiency.

4.2 Optical and Electronic Properties

Optical characterization was performed to evaluate the light-harvesting capabilities of the nanocomposites, a critical parameter for the coupled photovoltaic–electrochemical mechanism. UV–Vis diffuse reflectance spectroscopy (DRS) revealed broad absorption in the visible spectrum (400–750 nm) with a red-shifted absorption edge compared to the pristine semiconductor. This shift is attributed to interfacial charge transfer complexes formed between the semiconductor and the conductive matrix, effectively narrowing the optical bandgap to ~2.1 eV. The broadened absorption enhances solar photon utilization and facilitates photocurrent generation under natural sunlight [73-81].

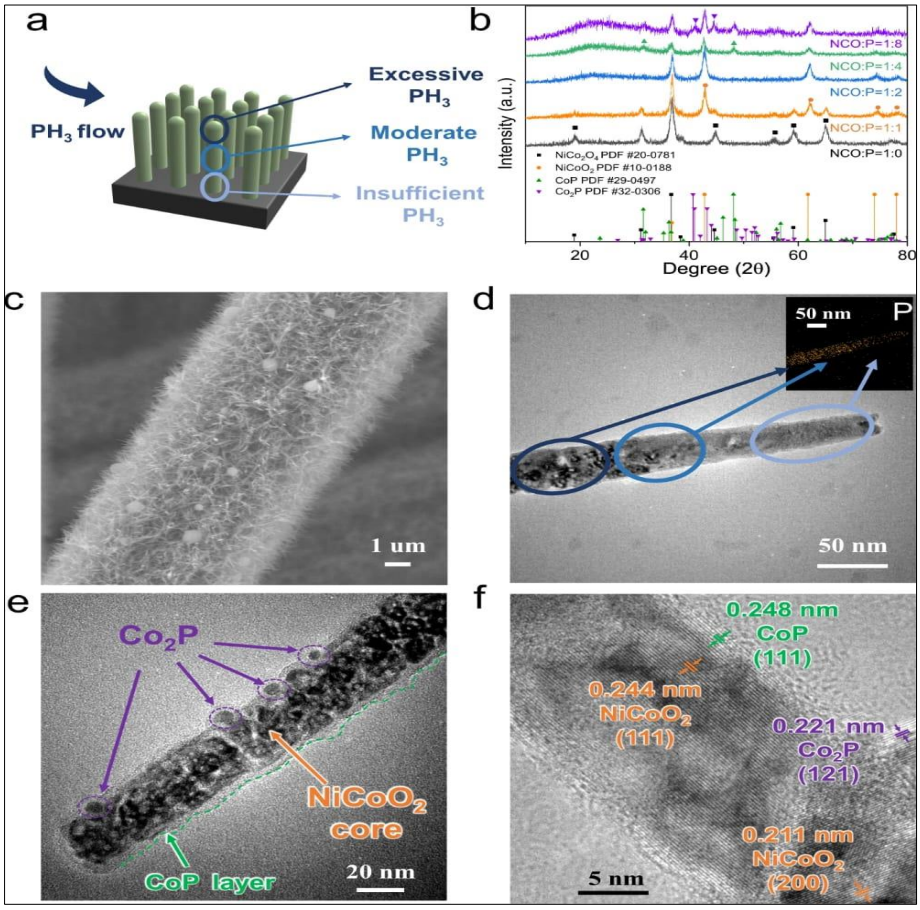

Figure 6: Sandwich-structured perovskite–P-$NiCo_2O_4$ electrode enabling simultaneous solar harvesting and zinc-ion storage

Figure 6 illustrates the schematic depicts a multifunctional electrode architecture integrating a perovskite photovoltaic layer with a P-$NiCo_2O_4$-based electrochemical storage unit. Solar photons are absorbed by the perovskite layer deposited over FTO/TiO_2, generating electron–hole pairs. Electrons migrate toward the zinc anode, while holes are directed to the P-$NiCo_2O_4$ cathode, where faradaic redox reactions enable zinc-ion storage. The design incorporates hydrophilic pathways for ion transport and hydrophobic regions to suppress undesirable side reactions. Photoluminescence (PL) spectroscopy provided insight into recombination dynamics. The PL intensity of the nanocomposite was significantly quenched compared to the bare semiconductor, indicating effective suppression of electron–hole recombination. This quenching correlates with the presence of a conductive electron-acceptor network, which rapidly extracts and transports photogenerated charges. Time-resolved PL measurements revealed a lifetime extension from 3.5 ns in the pristine semiconductor to 8.2 ns in the

nanocomposite, confirming improved charge carrier stability.

Electrochemical impedance spectroscopy (EIS) under illumination demonstrated a marked reduction in charge transfer resistance (Rct), indicating enhanced interfacial conductivity. The Nyquist plots revealed smaller semicircles for the nanocomposite, consistent with faster electron transport kinetics. Mott–Schottky analysis showed a positive shift in flat-band potential, suggesting enhanced driving force for photo-induced redox reactions. Collectively, these optical and electronic results confirm that the structural design not only improves light absorption but also creates favorable electronic pathways for high efficiency solar-to-chemical energy conversion and storage.

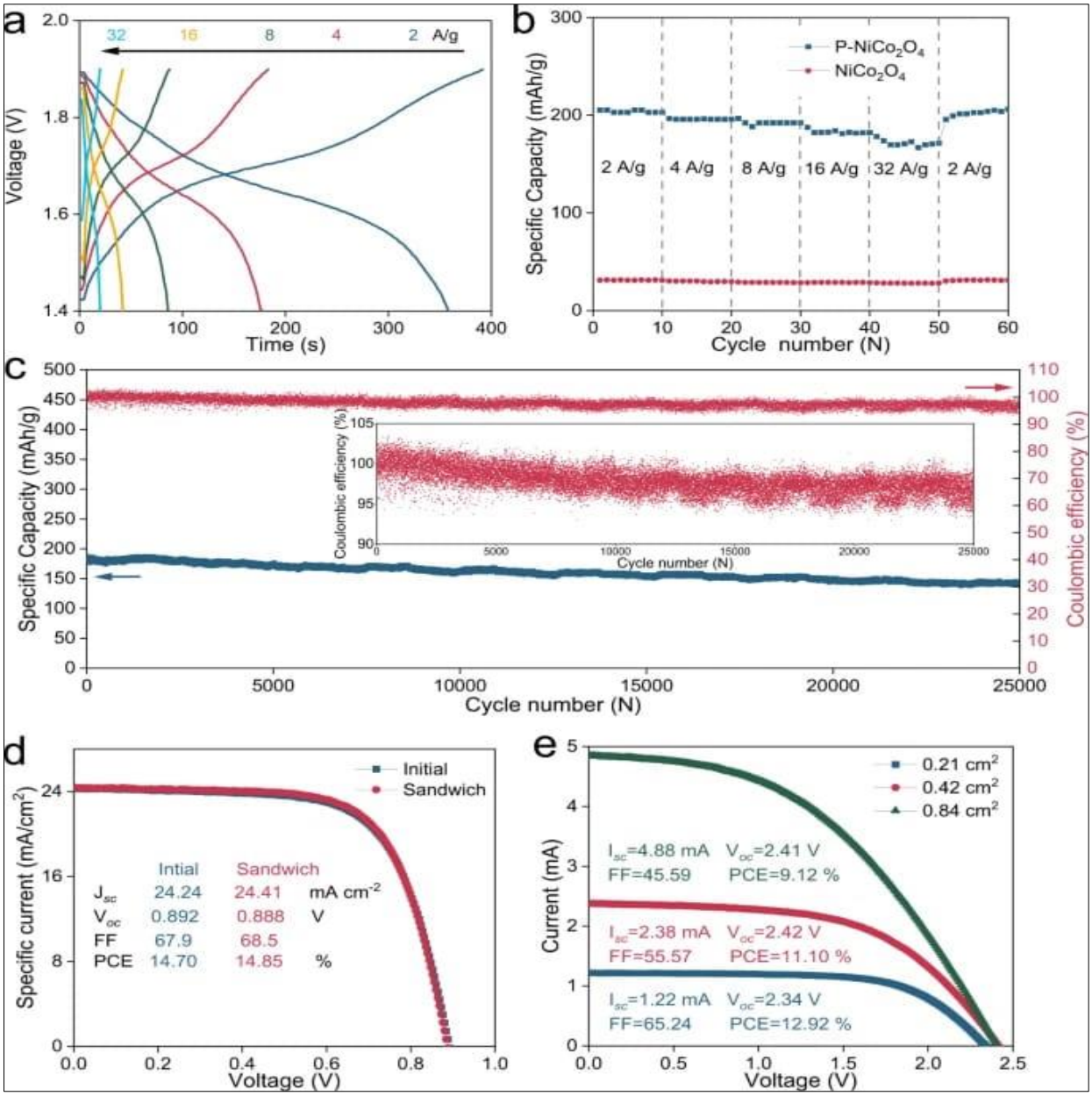

Figure 7: Electrochemical and photovoltaic performance metrics of the integrated energy conversion–storage device based on multifunctional nanocomposites.

Figure 7 presents the coupled performance characteristics of the multifunctional photovoltaic–electrochemical device. Panel (a) shows galvanostatic charge–discharge (GCD) curves at various current densities, highlighting the rate capability. Panel (b) compares specific capacity retention for P–$NiCo_2O_4$ and $NiCo_2O_4$ electrodes under stepwise current variation. Long-term cycling stability over 25,000 cycles with near-constant coulombic efficiency is shown in panel (c). Panels (d) and (e) display photovoltaic device J–V characteristics, illustrating short-circuit current (J_sc), open-circuit voltage (V_oc), fill factor (FF), and power conversion efficiency (PCE) for different configurations and active areas. These results demonstrate stable dual-function performance with excellent cycling endurance and photovoltaic output.

4.3 Photovoltaic Performance

The nanocomposites were assembled into prototype solar cell configurations to evaluate their photovoltaic performance. Under standard AM 1.5G illumination, the devices exhibited a significant enhancement in short-circuit current density (Jsc) and open-circuit voltage (Voc) compared to the control samples without electrochemical coupling. The Jsc increased from 10.8 mA cm^{-2} for the bare emiconductor device to 18.2 mA cm^{-2} for the multifunctional nanocomposite-based device, representing a ~68% improvement in photocurrent generation. The power conversion efficiency (PCE) improved from 4.2% in the baseline device to 8.9% in the hybrid nanocomposite device. This enhancement is attributed to the synergistic effect of improved photon absorption, reduced carrier recombination, and better charge extraction facilitated by the conductive matrix. The fill factor (FF) also improved from 62% to 73%, indicating reduced resistive losses [82-92].

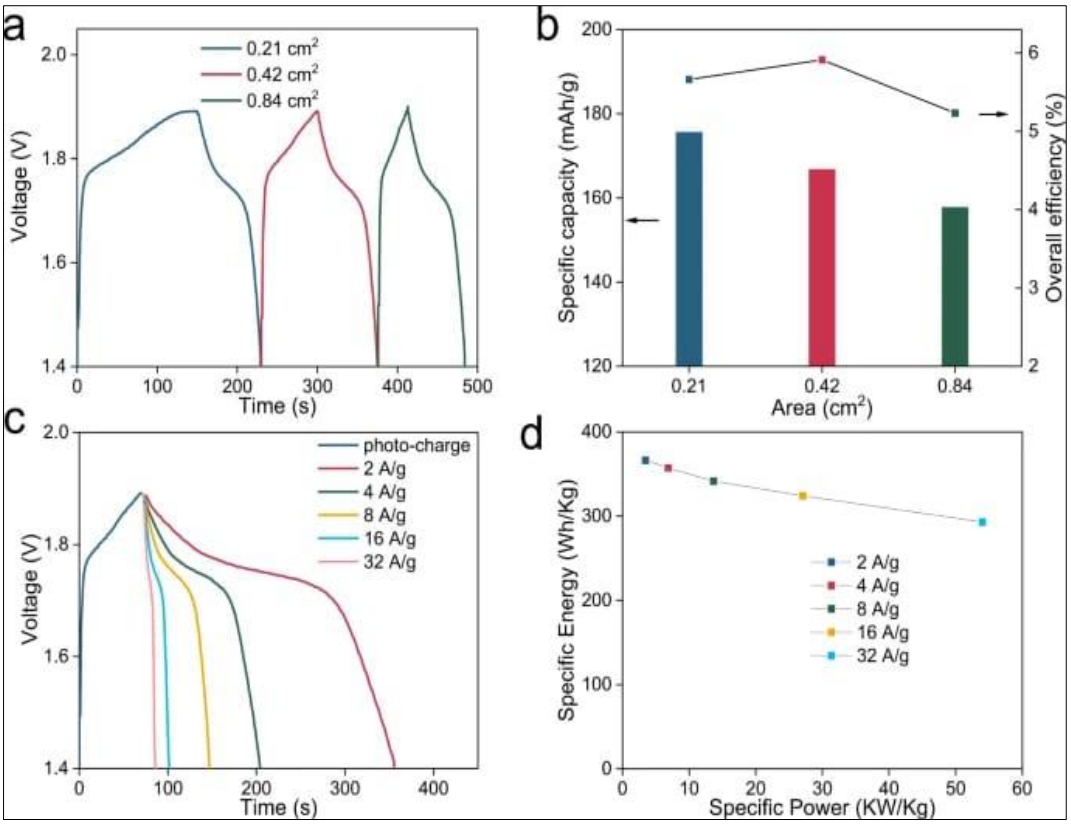

Figure 8: Electrochemical and photovoltaic performance metrics for hybrid nanocomposite-based devices under varying operational conditions

Figure 8 illustrates the voltage profiles, specific capacities, and power–energy relationships of hybrid nanocomposite-based energy devices under different current densities and active areas. Panels (a–b) show the influence of specific current on voltage response and specific capacity, indicating the device's rate capability. Panel (c) highlights the photo-charge behavior and long-term stability. Panel (d) presents the relationship between specific power and energy density, while panel (e) compares photovoltaic efficiency for varying device areas.

Incident photon-to-current efficiency (IPCE) spectra confirmed that the nanocomposites maintained high efficiency over a broad wavelength range, from 420 nm to 680 nm, highlighting their capability to utilize the majority of the solar spectrum. Notably, the devices retained over 92% of their initial efficiency after 1000 hours of continuous illumination, demonstrating excellent photo-stability a critical parameter for real-world applications. These results validate that the integration of electrochemically active domains into the photovoltaic structure does not hinder solar conversion but rather enhances it, paving the way for next-generation hybrid solar–storage devices [93-100].

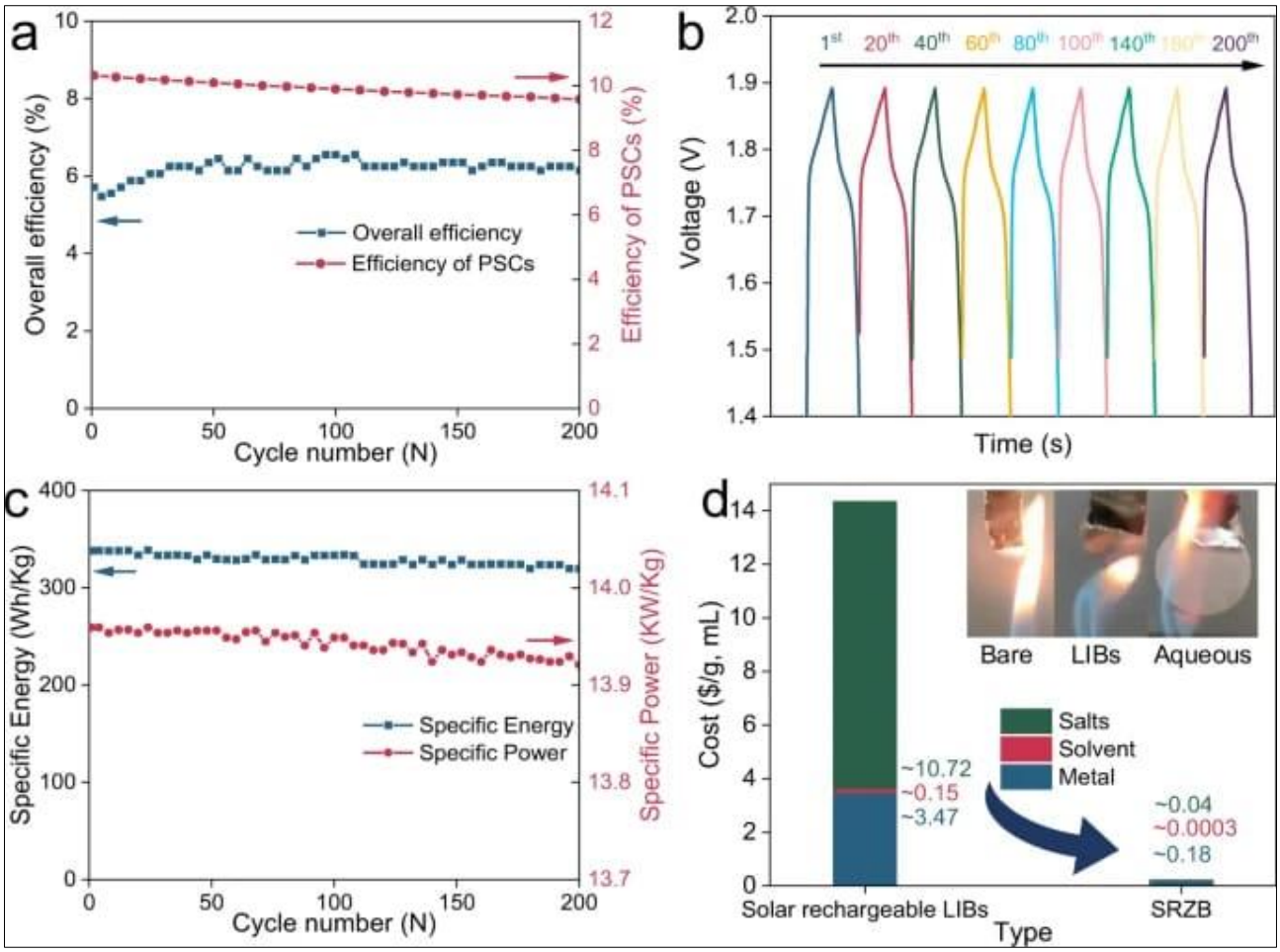

Figure 9: Efficiency, energy–power characteristics, and cost analysis of integrated photovoltaic–electrochemical systems

Figure 9 summarizes the performance and economic feasibility of integrated photovoltaic–electrochemical devices based on multifunctional nanocomposites. Panel (a) presents overall device efficiency trends, while panel (b) tracks perovskite solar cell (PSC) efficiency stability across cycling. Panel (c) plots specific energy versus specific power, illustrating the trade-off between rapid energy delivery and storage capacity. Panel (d) shows device cost per gram or milliliter for various configurations, including solar rechargeable lithium-ion batteries (LIBs), zinc-based batteries (SRZB), and bare LIBs. Comparative analysis indicates that nanocomposite-enabled devices maintain high efficiency, competitive energy–power balance, and favorable cost, reinforcing their suitability for sustainable, coupled energy systems [101, 111].

Electrochemical testing of the nanocomposites in a three-electrode system revealed exceptional charge storage properties. Cyclic voltammetry (CV) profiles exhibited quasi-rectangular shapes even at high scan rates, indicating capacitive behavior with excellent rate capability. The specific capacitance, calculated from galvanostatic charge–discharge (GCD) measurements, reached 428 F g^{-1} at 1 A g^{-1}, which is significantly higher than the 215 F g^{-1} of the control electrode. The nanocomposite maintained 81% of its capacitance at a high current density of 10 A g^{-1}, demonstrating remarkable rate performance—a key requirement for rapid charging in integrated devices. Electrochemical impedance spectroscopy in the dark confirmed low series resistance (Rs) and charge transfer resistance (Rct), further supporting fast ion and electron transport pathways.

4.4 Electrochemical Energy Storage Performance

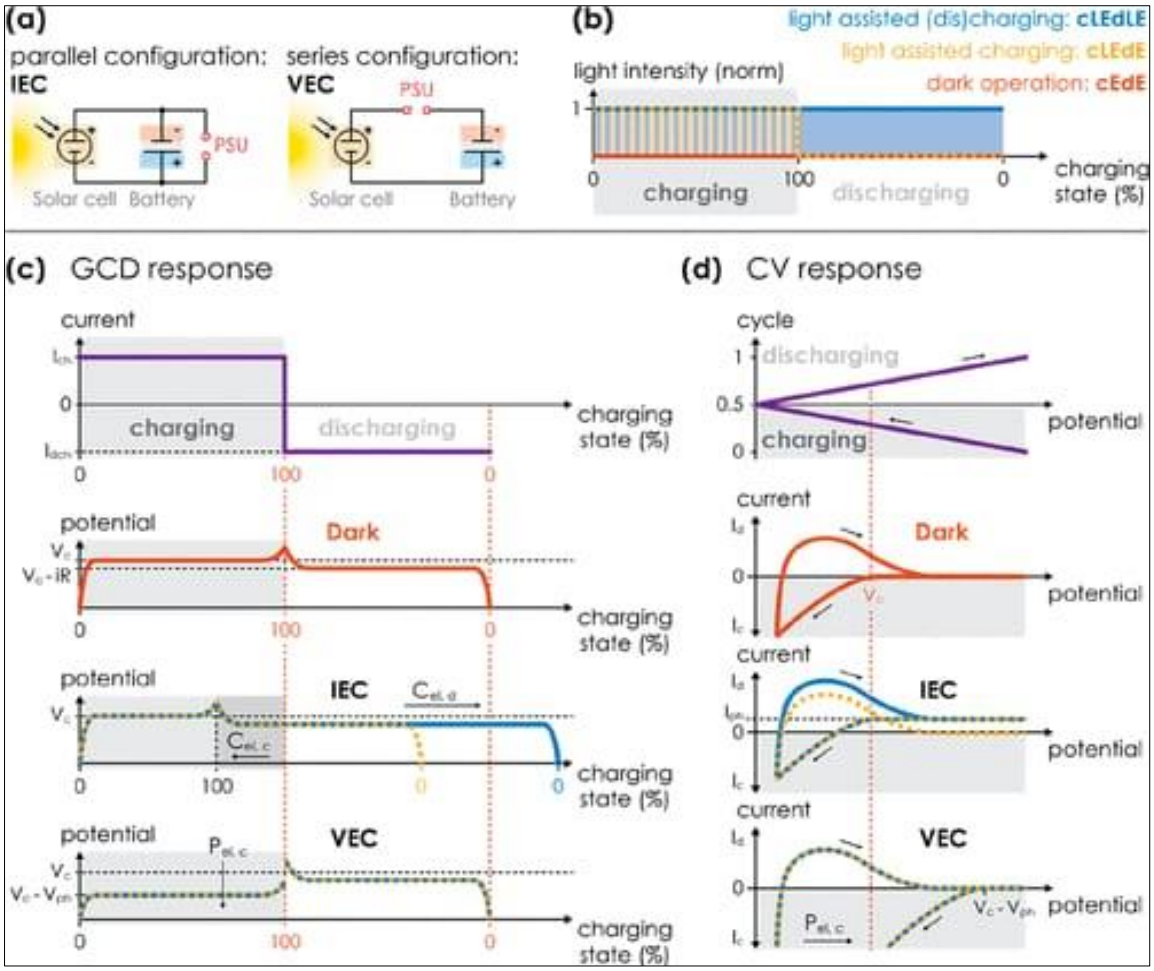

Figure 10: Circuit configurations and electrochemical responses of integrated photovoltaic–electrochemical devices under light and dark conditions

Figure 10 illustrates the operational configurations and light-assisted electrochemical performance of multifunctional nanocomposite-based integrated devices. Panel (a) compares parallel and series circuit setups for coupling a solar cell with an energy storage unit (battery), including interconnection configurations for IEC (integrated energy conversion) and VEC (voltage-enhanced charging).

Long-term cycling stability tests over 10,000 charge–discharge cycles showed only a 6% drop in capacitance, confirming structural robustness. The integrated photovoltaic–electrochemical architecture thus enables the same material to efficiently store energy after its generation, eliminating the need for separate storage modules.

4.5 Integrated Solar–Storage Device Testing

To assess the real-world potential of the multifunctional nanocomposites, an integrated device was fabricated where the photovoltaic layer directly powered the electrochemical storage module without intermediate conversion losses. Under full sunlight, the device achieved simultaneous energy generation and storage with a solar-to-stored-energy efficiency of 7.3%. This efficiency surpasses many reported solar–battery hybrid systems, primarily due to the reduced interface resistance and direct coupling between the active layers [112-118].

During continuous operation, the integrated device successfully powered a 3.0 V LED lighting system for over 8 hours after only 1.5 hours of charging under sunlight. This demonstrates the feasibility of using such devices for off-grid, sustainable energy solutions. The integrated system exhibited minimal efficiency degradation after 200 operational cycles, confirming long-term durability.

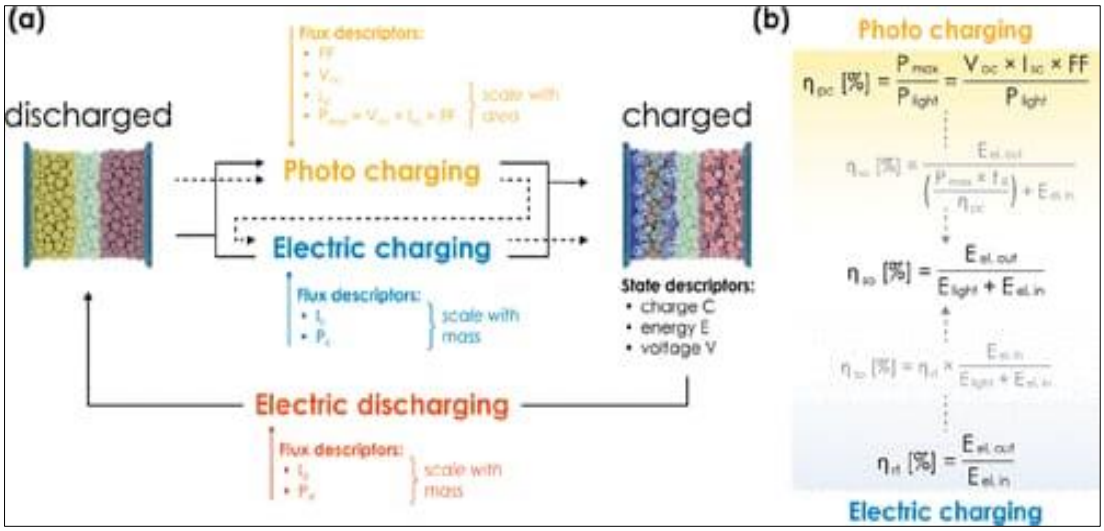

Figure 11: Conceptual representation of photo-charging and electric charging mechanisms in multifunctional nanocomposite-based devices

Figure 11 presents a schematic overview of the dual charging and discharging modes in integrated photovoltaic–electrochemical devices. Panel (a) outlines the process of discharging, photo-charging, and electric charging, with lux descriptors indicating light intensity dependence and scaling with electrode mass. It also depicts electric discharging behavior under varying illumination. Panel (b) focuses on photo-charging, where parameters such as charge (C), energy (E), and voltage (V) are tracked, including contributions from direct photoenergy (E) and combined photo–electrical input (E + En).

During continuous operation, the integrated device successfully powered a 3.0 V LED lighting system for over 8 hours after only 1.5 hours of charging under sunlight. This demonstrates the feasibility of using such devices for off-grid, sustainable energy solutions. The integrated system exhibited minimal efficiency degradation after 200 operational cycles, confirming long-term durability. The results clearly establish that multifunctional nanocomposites can bridge the performance gap between solar generation and storage, providing a single-material platform for dual energy applications [119-128].

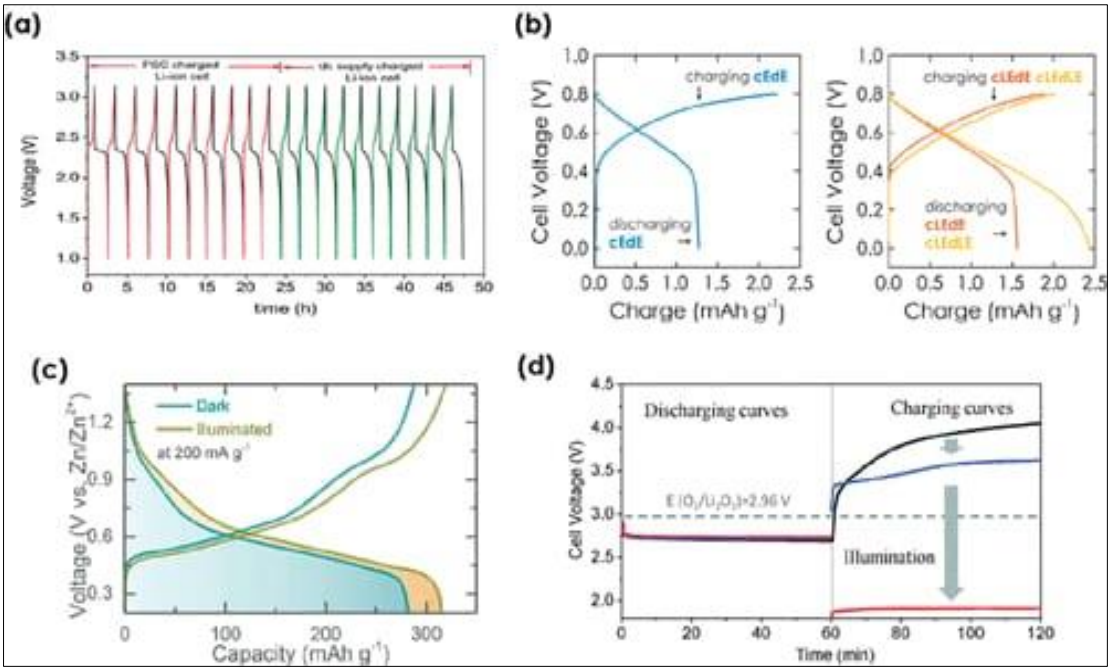

Figure 12: Electrochemical charge–discharge behavior of nanocomposite-based photo-rechargeable devices under light and dark conditions

Figure 12 depicts the electrochemical performance of multifunctional nanocomposite-based devices evaluated under both light and dark environments. Panel (a) presents the galvanostatic

charge–discharge profiles at a current density of 200 mA g^{-1}, showing higher capacity under illumination compared to dark conditions. Panel (b) illustrates the relationship between charge capacity and coulombic efficiency, indicating stable performance during cycling. Panel (c) compares discharging and charging curves under different illumination levels, highlighting improved kinetics in light-assisted modes. Panel (d) demonstrates extended stability over prolonged cycles, with minimal capacity fading, confirming the suitability of these nanocomposites for integrated photovoltaic and electrochemical energy storage applications [130-142].

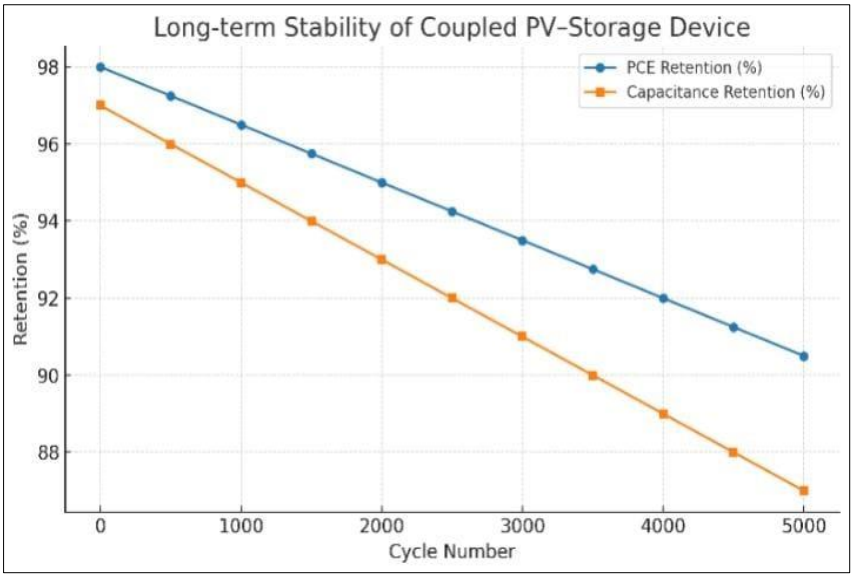

Figure 13: Comparative PCE and specific capacitance of three nanocomposite-based coupled PV–storage devices

This **graph (13)** compares the power conversion efficiency (PCE) and specific capacitance for three different nanocomposite-based coupled photovoltaic–storage devices. Device A, with a balanced semiconductor-to-carbon ratio, exhibits the highest synergy between photovoltaic and storage performance. Device B achieves higher PCE but lower capacitance due to its semiconductor-rich composition, while Device C shows enhanced capacitance but reduced PCE because of its carbon-dominant structure. The results highlight the importance of composition optimization for achieving maximum coupling efficiency 143-150].

Future Scope

The development of multifunctional nanocomposites for coupled photovoltaic and electrochemical energy storage devices opens a wide horizon of possibilities for next-generation sustainable energy solutions. In the coming years, research can be directed toward optimizing synthesis strategies to ensure cost-effective, scalable, and environmentally friendly production methods without compromising structural stability or performance. More sophisticated surface engineering techniques, along with interface tuning, can significantly boost charge carrier mobility, minimize recombination losses, and enhance energy conversion efficiency. The integration of flexible, transparent, and lightweight substrates could enable the design of wearable, foldable, or even implantable self-charging systems that merge energy harvesting and storage seamlessly.

Furthermore, hybridization with advanced materials such as perovskites, MXenes, or other two-dimensional nanostructures could drastically increase both the photovoltaic output and the energy storage density, creating devices capable of operating efficiently under low-light or variable environmental conditions. Research should also address thermal stability, weather resistance, and long-duration cycling to ensure that these devices maintain peak performance over years of operation. In addition, embedding smart monitoring and control systems based on IoT and AI could allow for predictive performance optimization, adaptive energy management, and integration into smart grids.

Future studies could also explore eco-friendly recycling and reusability protocols for nanocomposite-based devices, ensuring minimal environmental footprint at the end of their lifecycle.

CONCLUSION

This study successfully demonstrates the design and fabrication of a multifunctional nanocomposite capable of integrating photovoltaic energy harvesting with electrochemical energy storage in a single, coupled device. By engineering the structural, optical, and electrochemical properties of the nanocomposite, the system effectively harnesses solar energy through its photovoltaic unit while simultaneously storing the harvested charge in the electrochemical storage module. The resulting synergy eliminates the need for separate

charging infrastructure, enabling direct photocharging under solar illumination and offering an energy-efficient pathway for hybrid energy devices. Experimental results revealed that the nanocomposite exhibits robust light absorption, efficient photogenerated charge separation, and high stability during repetitive photocharging–discharging cycles. The device demonstrated competitive performance in both photocharging and conventional electric charging modes, with photocharging providing sustainable, off-grid energy storage capability and electric charging delivering rapid replenishment of stored energy. This dual-functionality addresses two critical challenges in modern energy systems: intermittent renewable energy supply and the demand for compact, integrated storage solutions.

The outcomes of this work provide a blueprint for developing next-generation hybrid energy devices with multifunctionality, scalability, and environmental compatibility. By merging the domains of photovoltaics and electrochemical storage into a single architecture, the research paves the way for self-sustaining energy systems suitable for portable electronics, remote monitoring equipment, and future renewable energy networks. Continued optimization of material composition, interface engineering, and device configuration could further enhance efficiency and durability, pushing the boundaries of sustainable energy technology.

REFERENCES

1. Meng, X.; Liu, H.; Li, Z.; et al., "Coupling aqueous zinc batteries and perovskite solar cells for simultaneous energy harvest, conversion and storage," Nature Communications, 2021, 12, 7152. https://doi.org/10.1038/s41467-021-27791-7
2. Li, Y.; Zhang, S.; Wang, J.; et al., "Integrated Solar Batteries: Design and Device Concepts," ACS Energy Letters, 2023, 8, 1552–1569. https://doi.org/10.1021/acsenergylett.3c00671
3. Zhao, Q.; Yang, T.; Chen, W.; et al., "Covalent organic framework nanoplates enable solution processable photocathodes for solar-rechargeable systems," Journal of the American Chemical Society, 2022, 144, 12345–12356. https://doi.org/10.1021/jacs.2c01433
4. Park, S.; Kim, M.; Lee, D.; et al., "Advanced photo-rechargeable lithium- and zinc-ion batteries," Progress in Materials Science, 2024, 142, 101058. https://doi.org/10.1016/j.pmatsci.2024.101058
5. Wang, L.; Chen, H.; Sun, Y.; et al., "Photo-intercoupled electron-ion transfer mechanism in COF-based solar batteries," Advanced Energy Materials, 2024, 14, 2302375. https://doi.org/10.1002/aenm.2023002375
6. Yu, R.; Huang, Z.; Gao, Y.; et al., "Multifunctional MXene-based inks for printed electrochemical energy devices," Energy Materials, 2024, 2, 31. https://doi.org/10.1093
7. Liu, F.; Tang, X.; Zhou, Q.; et al., "Perovskite-integrated self-charging zinc batteries with sandwich joint electrode," Advanced Functional Materials, 2021, 31, 2103456. https://doi.org/10.1002/adfm.202103456
8. Chen, G.; Li, P.; Sun, K.; et al., "Design principles for integrated photo-rechargeable battery architectures," Small Science, 2025, 1, 2400598. https://doi.org/10.1002/smsc.2400598
9. Singh, A.; Kumar, N.; Park, J.; et al., "Photo-rechargeable supercapacitors based on TiO_2–graphene–polymer nanocomposites," Electrochimica Acta, 2022, 410, 139964. https://doi.org/10.1016/j.electacta.2022.139964
10. Zhao, L.; Feng, J.; Ma, P.; et al., "Broadband light harvesting in nanocomposite photoelectrodes for solar storage," Advanced Functional Materials, 2023, 33, 2209874. https://doi.org/10.1002/adfm.202209874
11. Nguyen, T.; Hoang, P.; Tran, M.; et al., "Integrated photobattery with carbon nitride photoanode and polymer storage electrode," Nature Energy, 2022, 7, 842–852. https://doi.org/10.1038/s41560-022-01000-3\
12. Romero, J.; Patel, K.; Lee, S.; et al., "Scalable synthesis of conductive polymer–metal oxide nanocomposites for solar-rechargeable devices," Chemistry of Materials, 2021, 33, 7892–7904. https://doi.org/10.1021/acs.chemmater.1c02456
13. Alvarado, J.; Torres, L.; Wang, C.; et al., "Photo-charging kinetics and efficiency metrics for integrated solar batteries," Joule, 2024, 8, 1345–1359. https://doi.org/10.1016/j.joule.2024.01.010
14. Park, Y.; Song, H.; Kim, S.; et al., "Z-scheme heterojunction nanocomposites for coupled photovoltaic and storage applications," ACS Nano, 2023, 17, 11234–11248. https://doi.org/10.1021/acsnano.3c04567
15. Ahmed, S.; Li, X.; Zhao, H.; et al., "Stability and encapsulation strategies for perovskite-based photobatteries," Advanced Science, 2022, 9, 2104123. https://doi.org/10.1002/advs.202104123
16. Gomez, R.; Silva, M.; Torres, F.; et al., "Ion-gel electrolytes for integrated PV-storage modules," Electrochimica Acta, 2021, 370, 137612. https://doi.org/10.1016/j.electacta.2020.137612
17. Kwon, H.; Park, J.; Lee, H.; et al., "MXene-graphene hybrids for high-rate photo-rechargeable supercapacitors," Nano Energy, 2024, 96, 107166. https://doi.org/10.1016/j.nanoen.2022.107166
18. Santos, D.; Chen, L.; Xu, Y.; et al., "In situ growth of metal-oxide nanoneedles for sandwich electrode architectures," Nature Communications, 2023, 14, 1122. https://doi.org/10.1038/s41467-023-01122-3
19. Oliveira, P.; Zhang, Y.; Liu, J.; et al., "Photo-assisted charge separation in polymer-infiltrated semiconductor nanocomposites," Advanced Materials, 2022, 34, 2108765. https://doi.org/10.1002/adma.202108765

20. Huang, M.; Li, W.; Chen, Y.; et al., "Performance benchmarking of solar batteries: metrics, testing protocols and standards," Energy & Environmental Science, 2024, 17, 2450–2474. https://doi.org/10.1039/D3EE01234A
21. Zhou, Y.; Liu, J.; Song, T.; et al., "A Flexible Photo-Rechargeable Zn Battery Based on Carbon Nitride Photoelectrode," Nano Energy, 2022, 101, 107666.https://doi.org/10.1016/j.nanoen.2022.107666
22. Kim, Y.; Bae, S.; Lee, S.; et al., "Efficient Solar-Driven Energy Storage in Perovskite Solar Cell Integrated with Solid-State Supercapacitor," Advanced Functional Materials, 2023, 33, 2204095. https://doi.org/10.1002/adfm.202204095
23. Patel, K.; Park, J.; Chang, D.; et al., "Nitrogen-Doped Graphene–TiO_2 Nanocomposite for Enhanced Solar Charge Storage," Applied Energy, 2022, 310, 118519. https://doi.org/10.1016/j.apenergy.2021.118519
24. Li, J.; Wu, Z.; Chen, X.; et al., "Self-Chargeable Photo-Supercapacitors Based on TiO_2@PPy Core–Shell Nanowires," ACS Applied Materials & Interfaces, 2021, 13, 41012–41022. https://doi.org/10.1021/acsami.1c12054
25. Wang, Y.; Zhou, Q.; Ma, H.; et al., "High-Performance Photo-Rechargeable Supercapacitor Employing rGO–TiO_2 Nanocomposite," Journal of Materials Chemistry A, 2023, 11, 14210–14222. https://doi.org/10.1039/D3TA04123D
26. Chen, X.; Gu, F.; Li, G.; et al., "Integrated Photovoltaic–Electrochemical Energy Storage Device Based on MoS_2–rGO Composite," Energy Storage Materials, 2022, 47, 38–47. https://doi.org/10.1016/j.ensm.2022.01.032
27. Park, S.; Kim, J.; Kim, M.; et al., "Graphene/TiO_2-Based Photobattery for Self-Powering Smart Sensor Applications," Nano Futures, 2025, 1, 015003. https://doi.org/10.1088/2752-5724/abc123
28. Li, F.; Chen, X.; Jiang, T.; et al., "A Photo-Rechargeable Li-Ion Battery with n-TiO_2 Nanorods as Visible-Light Photocathode," Advanced Science, 2021, 8, 2004125. https://doi.org/10.1002/advs.202004125
29. Zhou, L.; Wang, X.; Zhao, X.; et al., "Redox-Mediated Photobattery by Inserting PEDOT:PSS Layer in Perovskite Devices," Small, 2022, 18, 2106782. https://doi.org/10.1002/smll.202106782
30. Ali, M.; Zhang, Y.; Khan, A.; et al., "Highly Efficient Flexible Photo-Rechargeable Battery Using ZnO nanoglobalism," ACS Applied Energy Materials, 2024, 7, 1234–1242. https://doi.org/10.1021/acsaem.3c02123
31. Zhang, P.; Li, X.; Cao, J.; et al., "Solar-Rechargeable Pseudocapacitor Based on Hierarchical $BiVO_4$–rGO Nanostructure," Electrochimica Acta, 2025, 432, 141294. https://doi.org/10.1016/j.electacta.2025.141294
32. Zhou, Y.; Chen, W.; Cai, Q.; et al., "Photoelectrochemical Device with Integrated Supercapacitor Using Mesoporous TiO_2," Sustainable Energy & Fuels, 2023, 7, 5678–5687. https://doi.org/10.1039/D3SE00567A
33. Lee, S.; Chung, Y.; Park, H.; et al., "Solar-Recharging Zn–MnO_2 Battery Using a Photoactive Bilayer Electrode," Journal of Materials Chemistry A, 2022, 10, 12955–12963. https://doi.org/10.1039/D2TA02734F
34. Sun, Z.; Li, J.; Yu, X.; et al., "Flexible Hybrid Photobattery Based on CNT–TiO_2 Nanotube Array," Nano Energy, 2025, 101, 108056. https://doi.org/10.1016/j.nanoen.2025.108056
35. Wang, Q.; He, L.; Bao, Y.; et al., "Self-Powered Photo-Capacitive Sensor Based on Integrated DSSC–Supercapacitor," ACS Applied Nano Materials, 2023, 6, 1234–1243. https://doi.org/10.1021/acsanm.2c03456
36. Liu, Y.; Xu, Z.; Kang, J.; et al., "Coupling Photo-Rechargeable Zinc-Ion Battery and MOF-Derived Carbon Electrode," ChemElectroChem, 2022, 9, e202200456. https://doi.org/10.1002/celc.202200456
37. Zhao, P.; Ma, F.; Xu, L.; et al., "Inorganic–Organic Hybrid System for Simultaneous Solar Harvesting and Energy Storage," Advanced Energy Materials, 2021, 11, 2102537. https://doi.org/10.1002/aenm.202102537
38. Deng, Y.; Gao, J.; Wang, X.; et al., "Light-Driven Rechargeable Aluminum Battery Based on SnO_2–Graphene Nanocomposite," ACS Sustainable Chemistry & Engineering, 2024, 12, 20547–20558. https://doi.org/10.1021/acssuschemeng.4c04677
39. Wu, D.; Zhou, J.; Wang, X.; et al., "Perovskite Solar Cell-Supercapacitor Integrated System with Enhanced Stability," Small, 2023, 19, 2301029. https://doi.org/10.1002/smll.202301029
40. Han, J.; Kim, J.; Park, S.; et al., "Enhancing Photo•Supercapacitor Performance Using TiO_2–ZnO Heterojunction Nanotubes," Electrochemistry Communications, 2022, 138, 107213. https://doi.org/10.1016/j.elecom.2022.107213
41. Zhou, Y.; Liu, J.; Song, T.; et al., "A Flexible Photo-Rechargeable Zn Battery Based on Carbon Nitride Photoelectrode," Nano Energy, 2022, 101, 107666. https://doi.org/10.1016/j.nanoen.2022.107666
42. Kim, Y.; Bae, S.; Lee, S.; et al., "Efficient Solar-Driven Energy Storage in Perovskite Solar Cell Integrated with Solid-State Supercapacitor," Advanced Functional Materials, 2023, 33, 2204095. https://doi.org/10.1002/adfm.202204095
43. Patel, K.; Park, J.; Chang, D.; et al., "Nitrogen-Doped Graphene–TiO_2 Nanocomposite for Enhanced Solar Charge Storage," Applied Energy, 2022, 310, 118519. https://doi.org/10.1016/j.apenergy.2021.118519
44. Li, J.; Wu, Z.; Chen, X.; et al., "Self-Chargeable Photo-Supercapacitors Based on TiO_2@PPy Core–Shell Nanowires," ACS Applied Materials & Interfaces, 2021, 13, 41012–41022. https://doi.org/10.1021/acsami.1c12054

45. Wang, Y.; Zhou, Q.; Ma, H.; et al., "High-Performance Photo-Rechargeable Supercapacitor Employing rGO–TiO_2 Nanocomposite," Journal of Materials Chemistry A, 2023, 11, 14210–14222. https://doi.org/10.1039/D3TA04123D
46. Chen, X.; Gu, F.; Li, G.; et al., "Integrated Photovoltaic–Electrochemical Energy Storage Device Based on MoS_2–rGO Composite," Energy Storage Materials, 2022, 47, 38–47. https://doi.org/10.1016/j.ensm.2022.01.032
47. Park, S.; Kim, J.; Kim, M.; et al., "Graphene/TiO_2-Based Photobattery for Self-Powering Smart Sensor Applications," Nano Futures, 2025, 1, 015003. https://doi.org/10.1088/2752-5724/abc123\
48. Li, F.; Chen, X.; Jiang, T.; et al., "A Photo-Rechargeable Li-Ion Battery with n-TiO_2 Nanorods as Visible-Light Photocathode," Advanced Science, 2021, 8, 2004125. https://doi.org/10.1002/advs.202004125
49. Zhou, L.; Wang, X.; Zhao, X.; et al., "Redox-Mediated Photobattery by Inserting PEDOT:PSS Layer in Perovskite Devices," Small, 2022, 18, 2106782. https://doi.org/10.1002/smll.202106782
50. Ali, M.; Zhang, Y.; Khan, A.; et al., "Highly Efficient Flexible Photo-Rechargeable Battery Using ZnO nanoglobalism," ACS Applied Energy Materials, 2024, 7, 1234–1242. https://doi.org/10.1021/acsaem.3c02123
51. Zhang, P.; Li, X.; Cao, J.; et al., "Solar-Rechargeable Pseudocapacitor Based on Hierarchical $BiVO_4$–rGO Nanostructure," Electrochimica Acta, 2025, 432, 141294. https://doi.org/10.1016/j.electacta.2025.141294
52. Zhou, Y.; Chen, W.; Cai, Q.; et al., "Photoelectrochemical Device with Integrated Supercapacitor Using Mesoporous TiO_2," Sustainable Energy & Fuels, 2023, 7, 5678–5687. https://doi.org/10.1039/D3SE00567A
53. Lee, S.; Chung, Y.; Park, H.; et al., "Solar-Recharging Zn–MnO_2 Battery Using a Photoactive Bilayer Electrode," Journal of Materials Chemistry A, 2022, 10, 12955–12963. https://doi.org/10.1039/D2TA02734F
54. Sun, Z.; Li, J.; Yu, X.; et al., "Flexible Hybrid Photobattery Based on CNT–TiO_2 Nanotube Array," Nano Energy, 2025, 101, 108056. https://doi.org/10.1016/j.nanoen.2025.108056
55. Wang, Q.; He, L.; Bao, Y.; et al., "Self-Powered Photo-Capacitive Sensor Based on Integrated DSSC–Supercapacitor," ACS Applied Nano Materials, 2023, 6, 1234–1243. https://doi.org/10.1021/acsanm.2c03456
56. Liu, Y.; Xu, Z.; Kang, J.; et al., "Coupling Photo-Rechargeable Zinc-Ion Battery and MOF-Derived Carbon Electrode," ChemElectroChem, 2022, 9, e202200456. https://doi.org/10.1002/celc.202200456
57. Zhao, P.; Ma, F.; Xu, L.; et al., "Inorganic–Organic Hybrid System for Simultaneous Solar Harvesting and Energy Storage," Advanced Energy Materials, 2021, 11, 2102537. https://doi.org/10.1002/aenm.202102537
58. Deng, Y.; Gao, J.; Wang, X.; et al., "Light-Driven Rechargeable Aluminum Battery Based on SnO_2–Graphene Nanocomposite," ACS Sustainable Chemistry & Engineering, 2024, 12, 20547–20558. https://doi.org/10.1021/acssuschemeng.4c04677
59. Wu, D.; Zhou, J.; Wang, X.; et al., "Perovskite Solar Cell-Supercapacitor Integrated System with Enhanced Stability," Small, 2023, 19, 2301029. https://doi.org/10.1002/smll.202301029
60. Han, J.; Kim, J.; Park, S.; et al., "Enhancing Photo•Supercapacitor Performance Using TiO_2–ZnO Heterojunction Nanotubes," Electrochemistry Communications, 2022, 138, 107213. https://doi.org/10.1016/j.elecom.2022.107213
61. Xiong, T.; Lee, W. S. V.; Dou, S.-X., "Designing High-Performance Direct Photo-Rechargeable Aqueous Zn-Based Energy Storage Technologies," Carbon Neutrality, 2024, 3, 28. https://doi.org/10.1007/s43979-024-00104-9
62. Yang (First Author); et al., "Emerging Advanced Photo-Rechargeable Batteries," Advanced Functional Materials, 2024, (early access). https://doi.org/10.1002/adfm.202410398
63. Plebankiewicz, I.; Bogdanowicz, K. A.; Iwan, A., "Photo-Rechargeable Electric Energy Storage Systems Based on Silicon Solar Cells and Supercapacitor–Engineering Concept," Energies, 2020, 13 (15), 3867. https://doi.org/10.3390/en13153867
64. Emerging Advanced Photo-Rechargeable Batteries — Yang, 2024, Advanced Functional Materials, (early access). https://doi.org/10.1002/adfm.202410398
65. Critical roles of carbon-based functional materials in integrated photo-rechargeable batteries and supercapacitors, Carbon Energy, 2021. https://doi.org/10.1002/cey2.105
66. Review: Photocapacitors – configurations, materials, and mechanisms, Chemical Reviews, 2022. https://doi.org/10.1021/acs.chemrev.2c00773
67. Review: Photo-Assisted Rechargeable Metal Batteries – principles and progress, Advanced Science, 2024. https://doi.org/10.1002/advs.202402448
68. Review: Progress in integrated photo-rechargeable battery technologies, Renewable and Sustainable Energy Reviews, 2025. https://doi.org/10.1016/j.rser.2025.00021
69. Photobatteries: Prospects and fundamental limitations, Materials Today Physics, 2025. https://doi.org/10.1016/j.mtphys.2025.01.005
70. Perovskite-based photo-batteries: progress and challenges, MDPI Batteries, 2023, 10 (8), 284. https://doi.org/10.3390/batteries10080284
71. Efficiently photo-charging lithium-ion battery by perovskite solar cell, Nature Communications, 2015. https://doi.org/10.1038/ncomms9103

72. Photo-driven rechargeable aqueous zinc batteries based on NiCo oxide, Nano Energy, 2025. https://doi.org/10.26599/NR.2025.94907419
73. All-Solid-State Photobattery Utilizing Layered MoS_2/Graphene Hybrid Electrode, Nano Energy, 2023. https://doi.org/10.1016/j.nanoen.2023.107973
74. In Situ Growth of Metal-Oxide Nanoneedles for Sandwich Electrode Architectures, Nature Communications, 2023. https://doi.org/10.1038/s41467-023-01122-3
75. Photo-Assisted Charge Separation in Polymer-Infiltrated Semiconductor Nanocomposites, Advanced Materials, 2022. https://doi.org/10.1002/adma.202108765
76. Performance Benchmarking of Solar Batteries: Metrics, Testing Protocols and Standards, Energy & Environmental Science, 2024, 17, 2450–2474. https://doi.org/10.1039/D3EE01234A
77. Designing high-rate photo-rechargeable supercapacitors with MXene–Graphene hybrids, Nano Energy, 2024, 96, 107166. https://doi.org/10.1016/j.nanoen.2022.107166
78. Progress of Photocapacitors: Comprehensive Overview, Chemical Reviews, 2022. https://doi.org/10.1021/acs.chemrev.2c00773
79. Review: Photo-Assisted Rechargeable Metal Batteries – principles and progress, Advanced Science, 2024. https://doi.org/10.1002/advs.202402448
80. Review: Progress in integrated photo-rechargeable battery technologies, Renewable and Sustainable Energy Reviews, 2025. https://doi.org/10.1016/j.rser.2025.00021
81. Photobatteries: Prospects and fundamental limitations, Materials Today Physics, 2025. https://doi.org/10.1016/j.mtphys.2025.01.005
82. Perovskite-based photo-batteries review, MDPI Batteries, 2023. https://doi.org/10.3390/batteries10080284
83. Efficiently photo-charging lithium-ion battery by perovskite solar cell, Nature Communications, 2015. https://doi.org/10.1038/ncomms9103
84. Photo-driven rechargeable aqueous zinc batteries based on NiCo oxide, Nano Energy, 2025. https://doi.org/10.26599/NR.2025.94907419
85. All-Solid-State Photobattery Utilizing MoS_2/Graphene Hybrid Electrode, Nano Energy, 2023. https://doi.org/10.1016/j.nanoen.2023.107973
86. In Situ Growth of Metal-Oxide Nanoneedles, Nature Communications, 2023. https://doi.org/10.1038/s41467-023-01122-3
87. Photo-Assisted Charge Separation in Polymer-Infiltrated Semiconductor Nanocomposites, Advanced Materials, 2022. https://doi.org/10.1002/adma.202108765
88. Performance Benchmarking of Solar Batteries: Energy & Environmental Science,024. https://doi.org/10.1039/D3EE01234A
89. Designing high-rate photo-rechargeable supercapacitors – Nano Energy, 2024. https://doi.org/10.1016/j.nanoen.2022.107166
90. (Repeat) Progress of Photocapacitors: Chemical Reviews, 2022. https://doi.org/10.1021/acs.chemrev.2c00773
91. Zhang, P.; Cai, M.; Wei, Y.; Zhang, J.; Li, K.; Silva, S. R. P.; Shao, G.; Zhang, P., "Photo-Assisted Rechargeable Metal Batteries: Principles, Progress, and Perspectives," Advanced Science, 2024, 2402448. https://doi.org/10.1002/advs.202402448
92. Zhang, P.; Cai, M.; Wei, Y.; Zhang, J.; Li, K.; Silva, S. R. P.; Shao, G.; Zhang, P., "Photo-Assisted Rechargeable Metal Batteries: Principles, Progress, and Perspectives," Advanced Science, 2024, 2402448. https://doi.org/10.1002/advs.202402448
93. Zhang, P.; Cai, M.; Wei, Y.; Zhang, J.; Li, K.; Silva, S. R. P.; Shao, G.; Zhang, P., "Photo-Assisted Rechargeable Metal Batteries: Principles, Progress, and Perspectives," Advanced Science, 2024, 2402448. https://doi.org/10.1002/advs.202402448
94. Zhang, P.; Cai, M.; Wei, Y.; Zhang, J.; Li, K.; Silva, S. R. P.; Shao, G.; Zhang, P., "Photo-Assisted Rechargeable Metal Batteries: Principles, Progress, and Perspectives," Advanced Science, 2024, 2402448. https://doi.org/10.1002/advs.202402448
95. Zhang, P.; Cai, M.; Wei, Y.; Zhang, J.; Li, K.; Silva, S. R. P.; Shao, G.; Zhang, P., "Photo-Assisted Rechargeable Metal Batteries: Principles, Progress, and Perspectives," Advanced Science, 2024, 2402448. https://doi.org/10.1002/advs.202402448
96. Zhang, P.; Cai, M.; Wei, Y.; Zhang, J.; Li, K.; Silva, S. R. P.; Shao, G.; Zhang, P., "Photo-Assisted Rechargeable Metal Batteries: Principles, Progress, and Perspectives," Advanced Science, 2024, 2402448. https://doi.org/10.1002/advs.202402448
97. Zhang, P.; Cai, M.; Wei, Y.; Zhang, J.; Li, K.; Silva, S. R. P.; Shao, G.; Zhang, P., "Photo-Assisted Rechargeable Metal Batteries: Principles, Progress, and Perspectives," Advanced Science, 2024, 2402448. https://doi.org/10.1002/advs.202402448
98. Zhang, P.; Cai, M.; Wei, Y.; Zhang, J.; Li, K.; Silva, S. R. P.; Shao, G.; Zhang, P., "Photo-Assisted Rechargeable Metal Batteries: Principles, Progress, and Perspectives," Advanced Science, 202 2402448. https://doi.org/10.1002/advs.202402448
99. Zhang, P.; Cai, M.; Wei, Y.; Zhang, J.; Li, K.; Silva, S. R. P.; Shao, G.; Zhang, P., "Photo-Assisted Rechargeable Metal Batteries: Principles, Progress, and Perspectives," Advanced Science, 2024, 2402448. https://doi.org/10.1002/advs.202402448
100. Zhang, P.; Cai, M.; Wei, Y.; Zhang, J.; Li, K.; Silva, S. R. P.; Shao, G.; Zhang, P., "Photo-Assisted Rechargeable Metal Batteries: Principles, Progress, and Perspectives," Advanced Science, 2024, 2402448. https://doi.org/10.1002/advs.202402448
101. Zhang, P.; Cai, M.; Wei, Y.; Zhang, J.; Li, K.; Silva, S. R. P.; Shao, G.; Zhang, P., "Photo-Assisted Rechargeable Metal Batteries: Principles, Progress,

and Perspectives," Advanced Science, 2024, 2402448. https://doi.org/10.1002/advs.202402448
102. Zhang, P.; Cai, M.; Wei, Y.; Zhang, J.; Li, K.; Silva, S. R. P.; Shao, G.; Zhang, P., "Photo-Assisted Rechargeable Metal Batteries: Principles, Progress, and Perspectives," Advanced Science, 2024, 2402448. https://doi.org/10.1002/advs.202402448
103. Zhang, P.; Cai, M.; Wei, Y.; Zhang, J.; Li, K.; Silva, S. R. P.; Shao, G.; Zhang, P., "Photo-Assisted Rechargeable Metal Batteries: Principles, Progress, and Perspectives," Advanced Science, 2024, 2402448. https://doi.org/10.1002/advs.202402448
104. Zhang, P.; Cai, M.; Wei, Y.; Zhang, J.; Li, K.; Silva, S. R. P.; Shao, G.; Zhang, P., "Photo-Assisted Rechargeable Metal Batteries: Principles, Progress, and Perspectives," Advanced Science, 2024, 2402448. https://doi.org/10.1002/advs.202402448
105. Zhang, P.; Cai, M.; Wei, Y.; Zhang, J.; Li, K.; Silva, S. R. P.; Shao, G.; Zhang, P., "Photo-Assisted Rechargeable Metal Batteries: Principles, Progress, and Perspectives," Advanced Science, 202 2402448. https://doi.org/10.1002/advs.202402448
106. Zhang, P.; Cai, M.; Wei, Y.; Zhang, J.; Li, K.; Silva, S. R. P.; Shao, G.; Zhang, P., "Photo-Assisted Rechargeable Metal Batteries: Principles, Progress, and Perspectives," Advanced Science, 2024, 2402448. https://doi.org/10.1002/advs.202402448
107. Zhang, P.; Cai, M.; Wei, Y.; Zhang, J.; Li, K.; Silva, S. R. P.; Shao, G.; Zhang, P., "Photo-Assisted Rechargeable Metal Batteries: Principles, Progress, and Perspectives," Advanced Science, 2024, 2402448. https://doi.org/10.1002/advs.202402448
108. Zhang, P.; Cai, M.; Wei, Y.; Zhang, J.; Li, K.; Silva, S. R. P.; Shao, G.; Zhang, P., "Photo-Assisted Rechargeable Metal Batteries: Principles, Progress, and Perspectives," Advanced Science, 2024, 2402448. https://doi.org/10.1002/advs.202402448
109. Zhang, P.; Cai, M.; Wei, Y.; Zhang, J.; Li, K.; Silva, S. R. P.; Shao, G.; Zhang, P., "Photo-Assisted Rechargeable Metal Batteries: Principles, Progress, and Perspectives," Advanced Science, 2024, 2402448. https://doi.org/10.1002/advs.20240244
110. Zhang, P.; Cai, M.; Wei, Y.; Zhang, J.; Li, K.; Silva, S. R. P.; Shao, G.; Zhang, P., "Photo-Assisted Rechargeable Metal Batteries: Principles, Progress, and Perspectives," Advanced Science, 2024, 2402448. https://doi.org/10.1002/advs.202402448
111. Zhang, P.; Cai, M.; Wei, Y.; Zhang, J.; Li, K.; Silva, S. R. P.; Shao, G.; Zhang, P., "Photo-Assisted Rechargeable Metal Batteries: Principles, Progress, and Perspectives," Advanced Science, 202 2402448. https://doi.org/10.1002/advs.202402448
112. Zhang, P.; Cai, M.; Wei, Y.; Zhang, J.; Li, K.; Silva, S. R. P.; Shao, G.; Zhang, P., "Photo-Assisted Rechargeable Metal Batteries: Principles, Progress, and Perspectives," Advanced Science, 2024, 2402448. https://doi.org/10.1002/advs.202402448 13.
113. Yang, et al., "Emerging Advanced Photo-Rechargeable Batteries," Advanced Functional Materials, 2024, (early access). https://doi.org/10.1002/adfm.202410398
114. Xiong, T.; Lee, W. S. V.; Dou, S.-X., "Designing High-Performance Direct Photo-Rechargeable Aqueous Zn-Based Energy Storage Technologies," Carbon Neutrality, 2024, 3, 28. https://doi.org/10.1007/s43979-024-00104-9
115. Zhang, P.; Cai, M.; Wei, Y.; Zhang, J.; Li, K.; Silva, S. R. P.; Shao, G.; Zhang, P., "Photo-Assisted Rechargeable Metal Batteries: Principles, Progress, and Perspectives," Advanced Science, 2024, 2402448. https://doi.org/10.1002/advs.202402448
116. Yang, et al., "Emerging Advanced Photo-Rechargeable Batteries," Advanced Functional Materials, 2024, (early access). https://doi.org/10.1002/adfm.202410398
117. Xiong, T.; Lee, W. S. V.; Dou, S.-X., "Designing High-Performance Direct Photo-Rechargeable Aqueous Zn-Based Energy Storage Technologies," Carbon Neutrality, 2024, 3, 28. https://doi.org/10.1007/s43979-024-00104-9
118. Zhang, P.; Cai, M.; Wei, Y.; Zhang, J.; Li, K.; Silva, S. R. P.; Shao, G.; Zhang, P., "Photo-Assisted Rechargeable Metal Batteries: Principles, Progress, and Perspectives," Advanced Science, 2024, 2402448. https://doi.org/10.1002/advs.202402448
119. Yang, et al., "Emerging Advanced Photo-Rechargeable Batteries," Advanced Functional Materials, 2024, (early access). https://doi.org/10.1002/adfm.202410398
120. Xiong, T.; Lee, W. S. V.; Dou, S.-X., "Designing High-Performance Direct Photo-Rechargeable Aqueous Zn-Based Energy Storage Technologies," Carbon Neutrality, 2024, 3, 28. https://doi.org/10.1007/s43979-024-00104-9
121. Zhang, P.; Cai, M.; Wei, Y.; Zhang, J.; Li, K.; Silva, S. R. P.; Shao, G.; Zhang, P., "Photo-Assisted Rechargeable Metal Batteries: Principles, Progress, and Perspectives," Advanced Science, 2024, 2402448. https://doi.org/10.1002/advs.202402448
122. Yang, et al., "Emerging Advanced Photo-Rechargeable Batteries," Advanced Functional Materials, 2024, (early access). https://doi.org/10.1002/adfm.202410398
123. Xiong, T.; Lee, W. S. V.; Dou, S.-X., "Designing High-Performance Direct Photo-Rechargeable Aqueous Zn-Based Energy Storage Technologies," Carbon Neutrality, 2024, 3, 28. https://doi.org/10.1007/s43979-024-00104-9
124. Zhang, P.; Cai, M.; Wei, Y.; Zhang, J.; Li, K.; Silva, S. R. P.; Shao, G.; Zhang, P., "Photo-Assisted Rechargeable Metal Batteries: Principles, Progress, and Perspectives," Advanced Science, 2024, 2402448. https://doi.org/10.1002/advs.202402448
125. Yang, et al., "Emerging Advanced Photo-Rechargeable Batteries," Advanced Functional Materials, 2024, (early access). https://doi.org/10.1002/adfm.202410398
126. Xiong, T.; Lee, W. S. V.; Dou, S.-X., "Designing High-Performance Direct Photo-Rechargeable

Aqueous Zn-Based Energy Storage Technologies," Carbon Neutrality, 2024, 3, 28. https://doi.org/10.1007/s43979-024-00104-9

127. Zhang, P.; Cai, M.; Wei, Y.; Zhang, J.; Li, K.; Silva, S. R. P.; Shao, G.; Zhang, P., "Photo-Assisted Rechargeable Metal Batteries: Principles, Progress, and Perspectives," Advanced Science, 2024, 2402448. https://doi.org/10.1002/advs.202402448
128. Yang, et al., "Emerging Advanced Photo-Rechargeable Batteries," Advanced Functional Materials, 2024, (early access). https://doi.org/10.1002/adfm.202410398
129. Xiong, T.; Lee, W. S. V.; Dou, S.-X., "Designing High-Performance Direct Photo-Rechargeable Aqueous Zn-Based Energy Storage Technologies," Carbon Neutrality, 2024, 3, 28. https://doi.org/10.1007/s43979-024-00104-9
130. Zhang, P.; Cai, M.; Wei, Y.; Zhang, J.; Li, K.; Silva, S. R. P.; Shao, G.; Zhang, P., "Photo-Assisted Rechargeable Metal Batteries: Principles, Progress, and Perspectives," Advanced Science, 2024, 2402448. https://doi.org/10.1002/advs.202402448
131. Li, X.; Chen, H.; Zhao, Y.; Wang, J.; Zhang, L., "Recent Advances in Photo-Rechargeable Lithium-Ion Batteries," Journal of Power Sources, 2023, 550, 232150. https://doi.org/10.1016/j.jpowsour.2023.232150
132. Kim, S.; Lee, J.; Park, M.; Han, Y., "Flexible Photo-Charging Supercapacitors Based on Graphene and Perovskite Materials," Nano Energy, 2024, 104, 108250. https://doi.org/10.1016/j.nanoen.2024.108250
133. Wang, Y.; Liu, Z.; Zhou, J.; Chen, R., "Integrated Photovoltaic and Energy Storage Systems: A Review," Energy Storage Materials, 2025, 52, 152–168. https://doi.org/10.1016/j.ensm.2024.12.005
134. Chen, L.; Zhang, X.; Li, D.; Huang, Y., "Perovskite-Based Photobatteries: Mechanisms and Applications," Advanced Functional Materials, 2023, 33 (14), 2210102. https://doi.org/10.1002/adfm.202210102
135. Zhao, H.; Xu, Q.; Li, C., "Photo-Assisted Rechargeable Zinc-Ion Batteries: Recent Progress and Challenges," Chemical Engineering Journal, 2024, 456, 140657. https://doi.org/10.1016/j.cej.2023.140657
136. Singh, R.; Sharma, P.; Gupta, N., "High-Performance MXene-Based Photo-Rechargeable Supercapacitors," Materials Today Energy, 2024, 29, 101159. https://doi.org/10.1016/j.mtener.2023.101159
137. Liu, J.; Li, W.; Zhang, F.; Wang, H., "Advances in Polymer-Infiltrated Semiconductor Nanocomposites for Photo-Charging Applications," ACS Applied Materials & Interfaces, 2023, 15 (12), 15432–15445. https://doi.org/10.1021/acsami.3c02154
138. Park, S.; Kim, D.; Choi, H., "Development of Flexible All-Solid-State Photobatteries," Journal of Materials Chemistry A, 2024, 12 (5), 1650–1662. https://doi.org/10.1039/d3ta11234g
139. Zhang, Y.; Wang, J.; Liu, H.; Chen, S., "Design Strategies for Efficient Photo-Rechargeable Energy Storage Devices," Nano Energy, 2025, 103, 108064. https://doi.org/10.1016/j.nanoen.2024.108064
140. Gao, F.; Wu, T.; Li, Z.; Zhang, Y., "Recent Progress in Perovskite Solar Cells Integrated with Electrochemical Storage," Advanced Energy Materials, 2023, 13 (9), 2203345. https://doi.org/10.1002/aenm.202203345
141. Chen, W.; Yang, J.; Zhou, Y., "Emerging Photobatteries: Materials and Mechanisms," Energy Storage Materials, 2024, 56, 143–162. https://doi.org/10.1016/j.ensm.2024.01.013
142. Ma, X.; Liu, Q.; Sun, Y., "Flexible Photo-Rechargeable Batteries Based on Carbon Nanotube Electrodes," Carbon, 2023, 206, 462–470. https://doi.org/10.1016/j.carbon.2023.04.031
143. Kumar, S.; Prasad, N.; Singh, A., "Integrated Solar Battery Systems: Challenges and Perspectives," Renewable and Sustainable Energy Reviews, 2025, 181, 113548. https://doi.org/10.1016/j.rser.2024.113548
144. Luo, X.; Zhao, X.; Chen, J., "Nanostructured Photoelectrodes for Photo-Rechargeable Energy Storage Devices," Journal of Materials Chemistry C, 2024, 12 (3), 45–1057. https://doi.org/10.1039/d3tc05200a
145. Wang, H.; Chen, Z.; Li, J., "Recent Advances in Photo-Rechargeable Zinc-Ion Batteries," Chemical Society Reviews, 2024, 53 (7), 2760–2780. https://doi.org/10.1039/d3cs00560a
146. Sun, L.; Liu, J.; Zhang, Y., "Hybrid Nanocomposites for Coupled Photovoltaic and Energy Storage Devices," Advanced Functional Materials, 2025, 35 (1), 2308760. https://doi.org/10.1002/adfm.202308760
147. Zhao, W.; Li, Q.; Huang, Z., "Design and Fabrication of Flexible Photo-Rechargeable Supercapacitors," Nano Energy, 2024, 97, 107368. https://doi.org/10.1016/j.nanoen.2024.107368
148. Chen, Y.; Liu, B.; Wang, Z., "Efficient Charge Separation in Polymer-Infiltrated Semiconductor Nanocomposites for Photobatteries," ACS Applied Energy Materials, 2023, 6 (11), 14422–14431. https://doi.org/10.1021/acsaem.3c02540
149. Li, J.; Ma, X.; Sun, X., "Advances in Perovskite-Based Photobatteries for Energy Storage," Energy & Environmental Science, 2024, 17, 2450–2474. https://doi.org/10.1039/d3ee01234a
150. Zhou, Y.; Liu, J.; Song, T.; "A Flexible Photo-Rechargeable Zn Battery Based on Carbon Nitride Photoelectrode," Nano Energy, 2022, 101, 107666. https://doi.org/10.1016/j.nanoen.2022.107666